Blast Scaling

Explosion Effects on Equipment, Structures, People and the Environment

Dr Arief Dahoe

Explosion, Hydrogen Safety and Combustion Scientist



Dutch Armed Forces

Knowledge Center for Explosion and Hydrogen Safety

http://www.explosionsolutions.org/kcehs/

ACKNOWLEDGEMENTS

UNIVERSITY OF CAMBRIDGE

TU Delft

Delft University of Technology

METHODS FOR THE EVALUATION OF BLAST EFFECTS

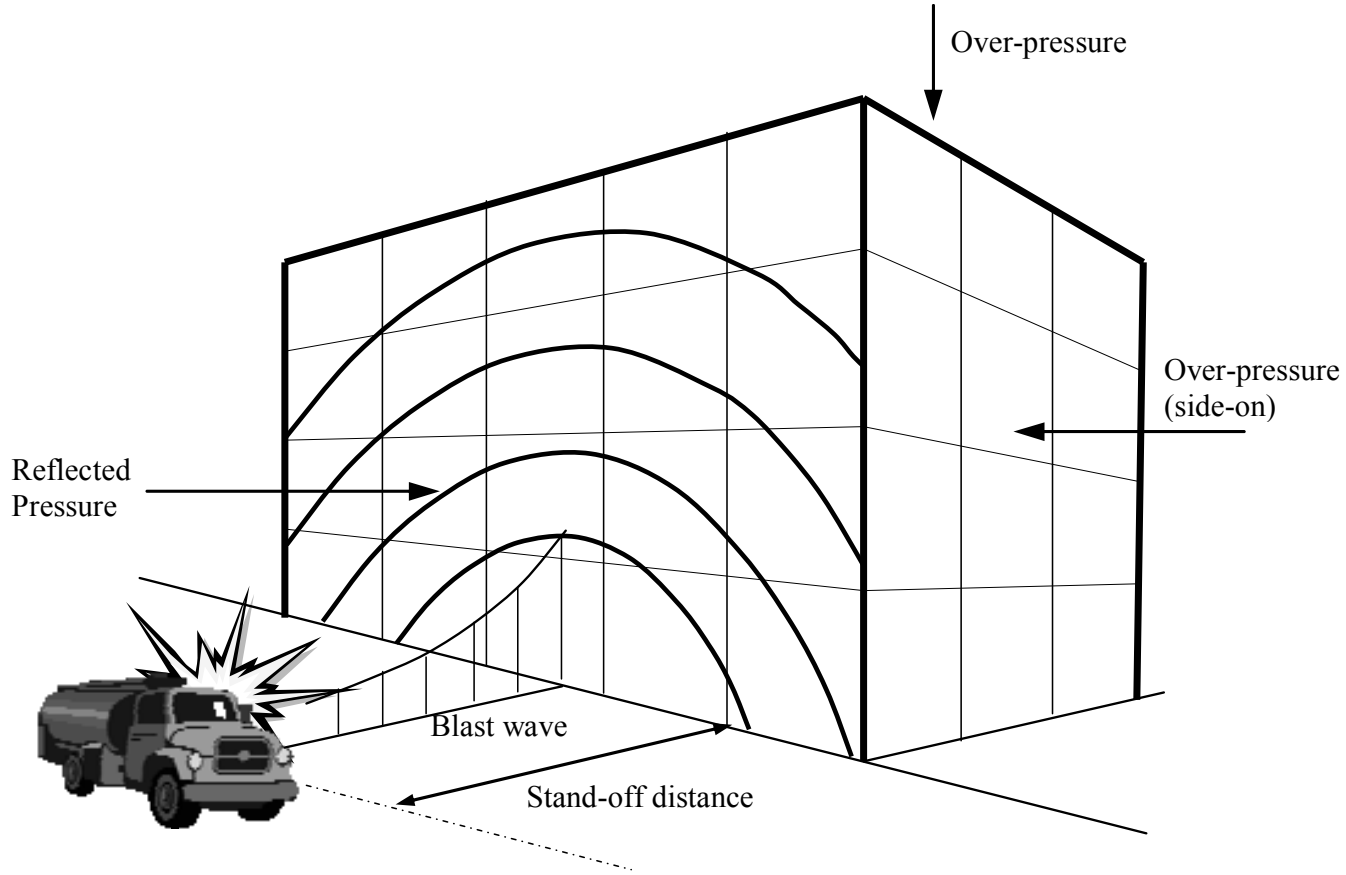
Method	Assumption	Limitations/Challenges
TNT equivalency	Blast propagation in idealised environment Obstacles not considered	The TNT equivalency model is not recommended as a method for modelling hydrogen explosions. The TNT equivalency method overestimates the overpressures in the near-field and converges to accurate values in the far-field. The method also does not consider plant geometry in its calculations. Furthermore, the pressure vs time profile obtained is different to what would be expected for a VCE, resulting in this method being more suitable for condensed phase explosions, which is not the case for hydrogen
Multi-energy (ME)	Contribution of congested zones to blast generation	Selection of initial blast strength according to degree of congestion
Baker-Strehlow-Tang (BST) method	Contribution of congested zones to blast generation	Specification of Mach number Sometimes underpredicts the explosion
Congestion Assessment Method (CAM)	Contribution of congested zones to blast generation	Applied only for unconfined congested regions (50-60% enclosed)

Source: Hydrohub Innovation Program. Safety aspects of green hydrogen production on industrial scale. Public Report, Institute for Sustainable Process Technology, The Netherlands, November 2023. [10].

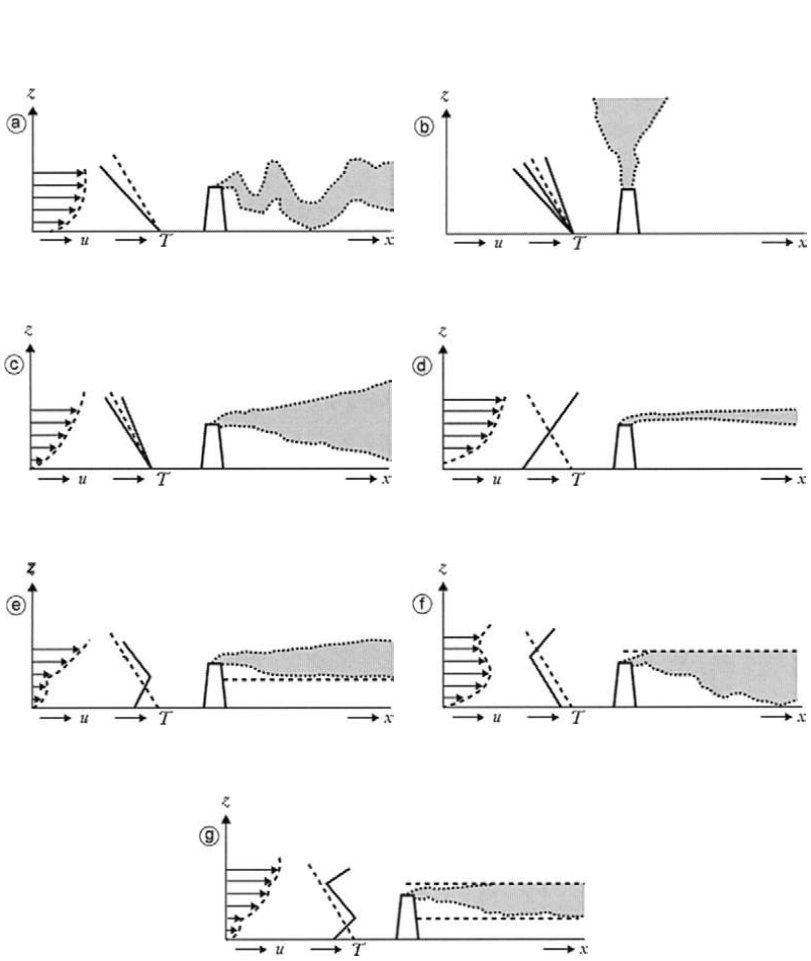
• Methods and models:
TNT Equivalency Method [2, 7], Multi Energy Method [11], Baker-Strehlow-Tang Method [8, 12], SCOPE-model [13] and the Congestion Assessment Method [14].

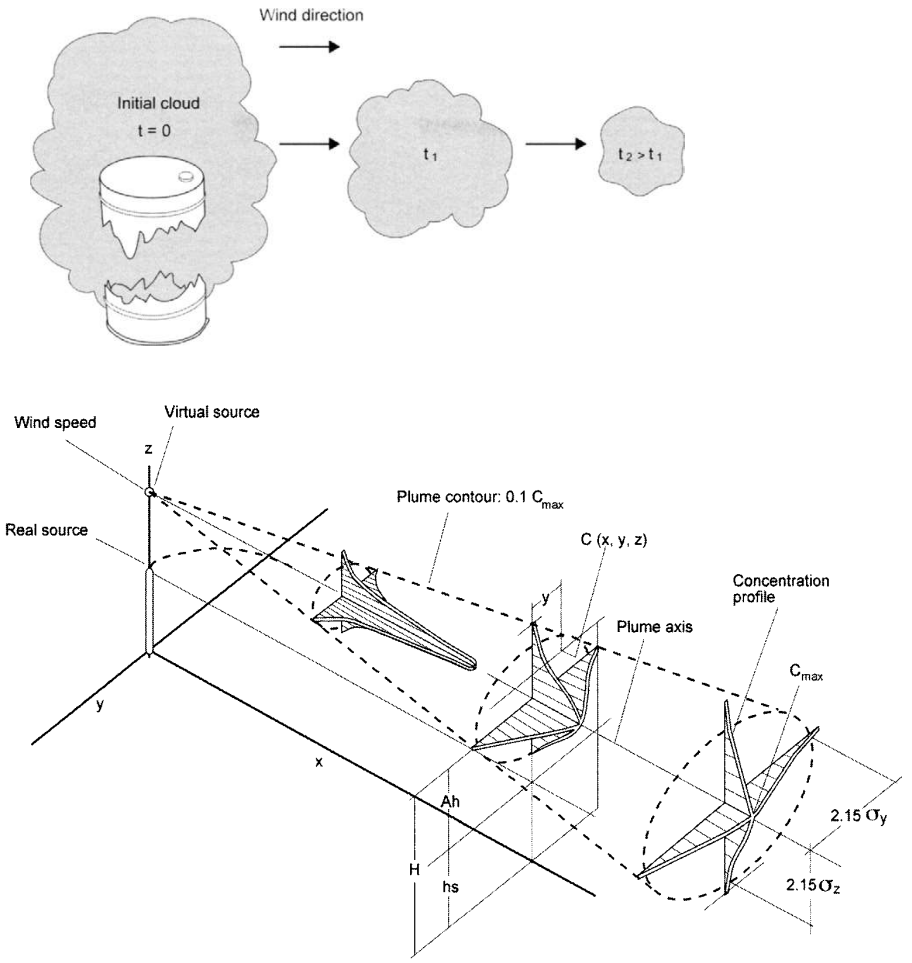
• Methods and models are incorporated into commercial software:
PHAST, SAFETI, SHELL FRED, SCOPE [13], EFFECTS, FLACS, KFX, and EXIM.

• The latest version of SHELL FRED deploys the model in Ref. [15].



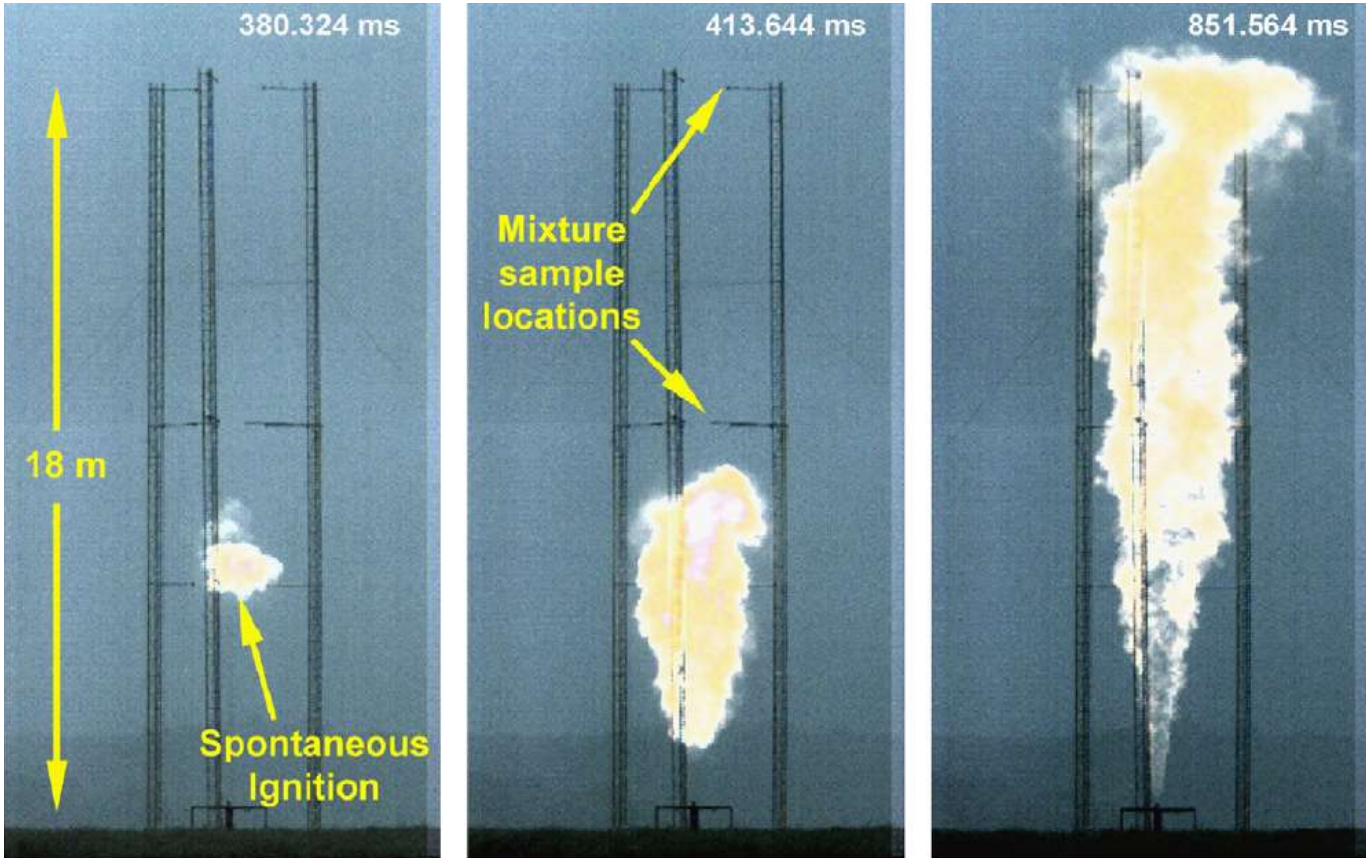
Unconfined explosion: Blast-structure interaction [1].



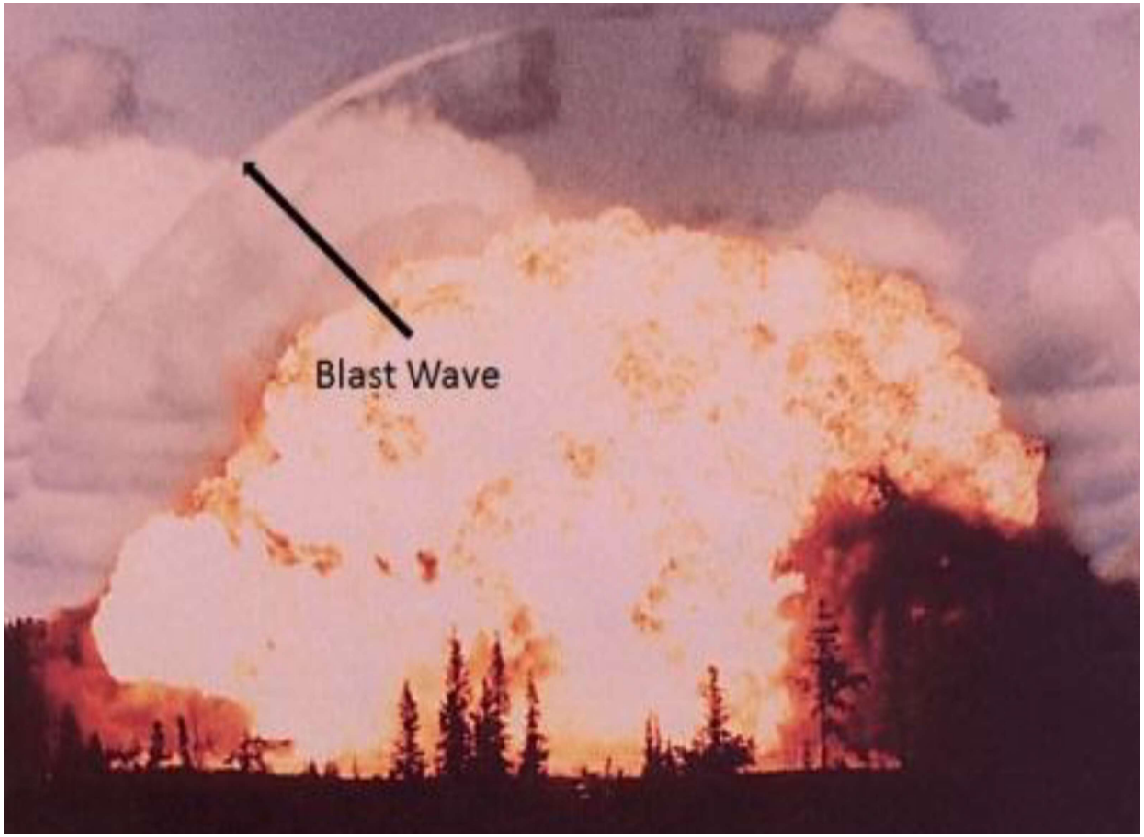


Plume rise due to momentum and buoyancy. Concentration distribution from a vented plume [2].

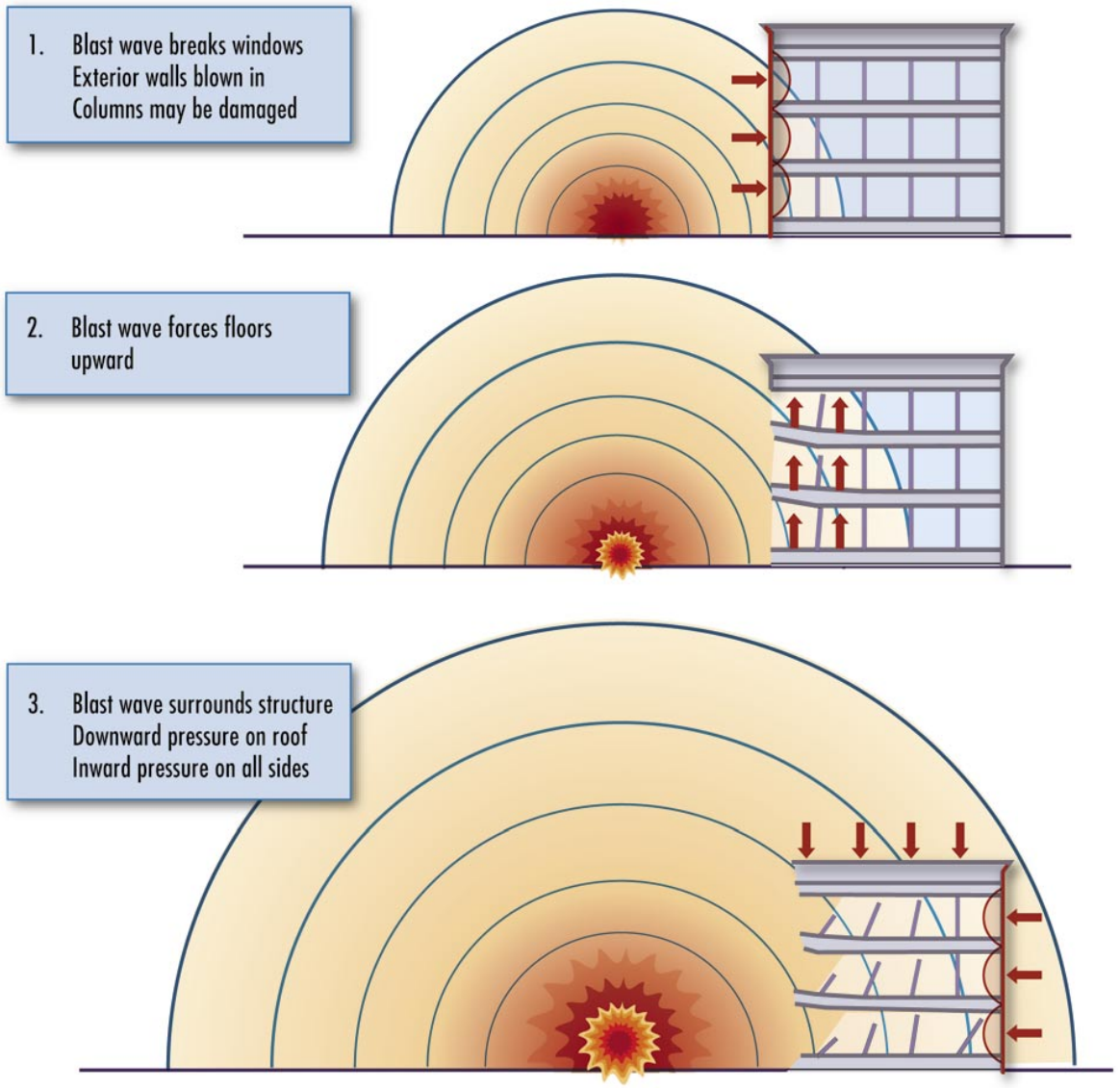
Jet fire formation during large scale hydrogen releases [3].



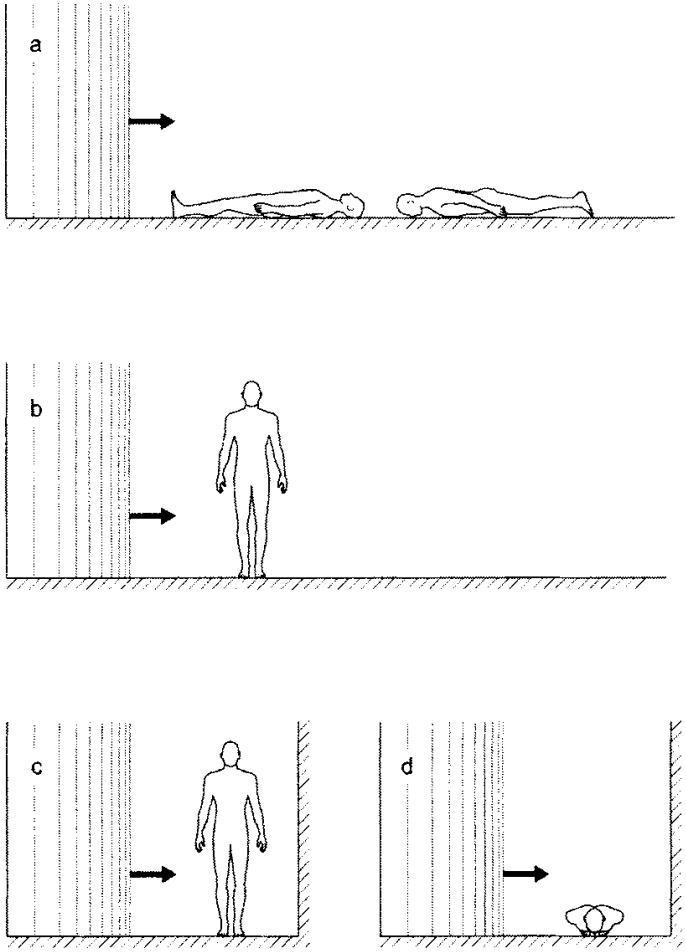
Vessel with a volume of 16.2 m^3; pressure: 24 bar.
Orifice/nozzle diameter: 42 mm.
Outflow: 27 kg H_2 released in 30 seconds.



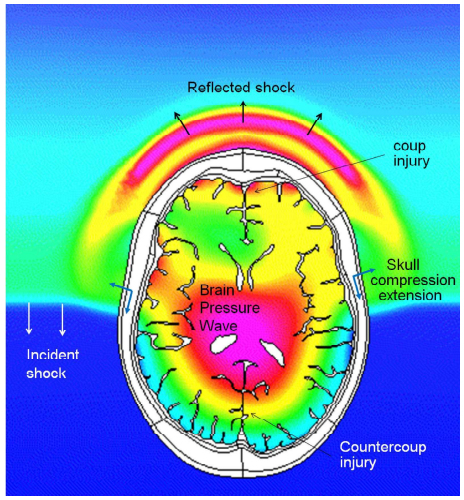
Blast wave formation.

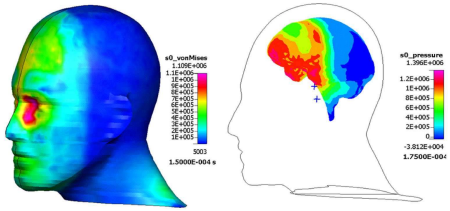


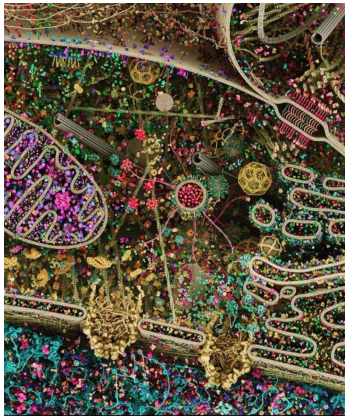
Blast pressure effects on a structure [4].

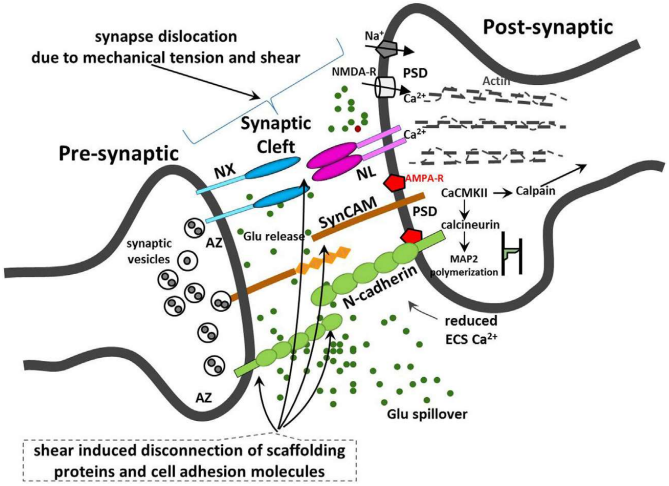


Injury due to blast effects [2, 5, 6].

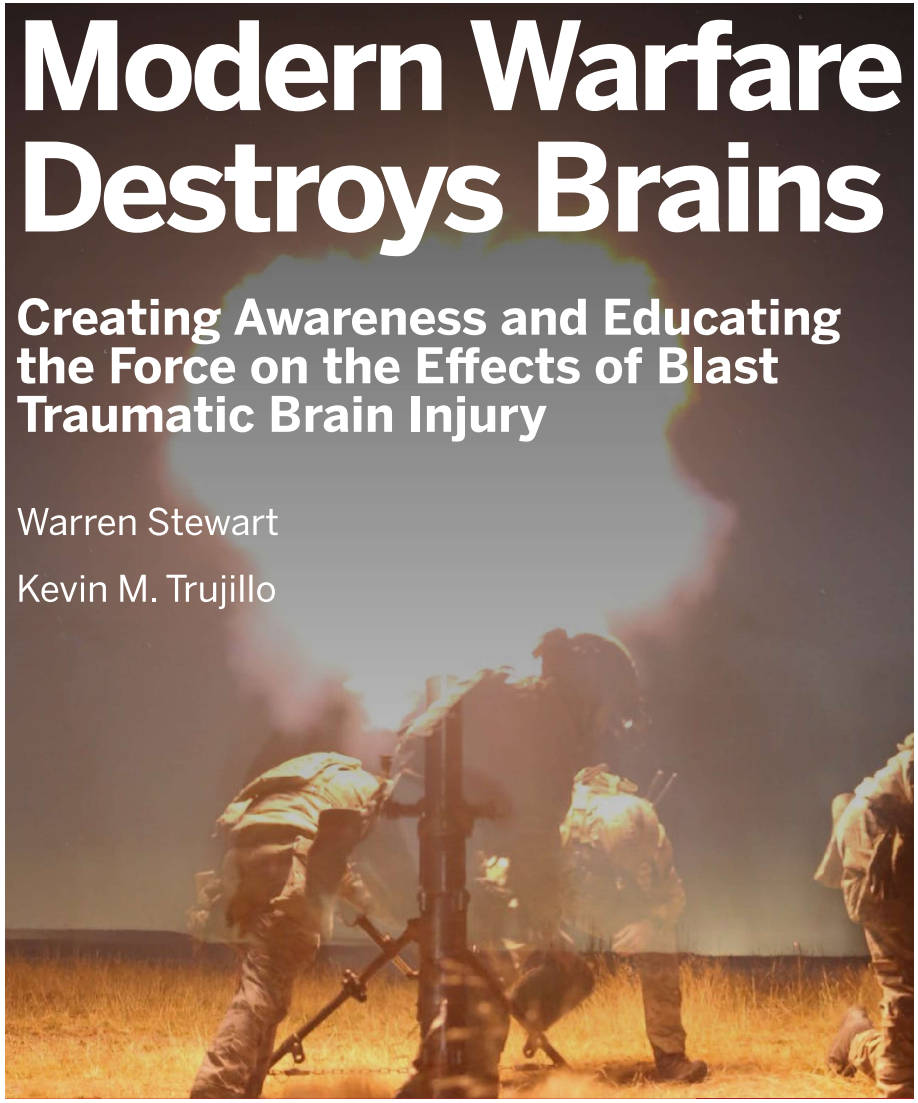








Cellular cross-section


Modern Warfare Destroys Brains
Creating Awareness and Educating the Force on the Effects of Blast Traumatic Brain Injury
Warren Stewart
Kevin M. Trujillo



Entry	**Overpressure** (kPa)	**Damage/injury**
1	190	Occupants of unstrengthened building will be killed by direct action of blast, by being struck by building debris, or by impact against hard surfaces [7].
2	69–76	Occupants of unstrengthened building are expected to suffer severe injuries or death from direct blast, building collapse, or translation [7].
3	70	Probable total destruction of buildings; heavy machine tools moved and badly damaged [2].
4	60	Loaded train boxcars completely demolished [2].
5	55	Occupants of unstrengthened building will be killed or incur serious injuries by blast to eardrums and lungs, by being blown down or struck by fragments and building debris [7].
6	50–55	Unreinforced brick panels, 25–35 cm thick, fail by shearing or flexure [2].
7	50	Loaded tank cars/train wagons overturned; brick walls, 20–30 cm thick, collapse [2].
8	40–45	Collapse of pipe bridge [2].
9	35–40	Displacement of pipe bridge, failure of piping [2].
10	20–40	Large trees fall down [2].
11	35	Breakage of wooden telephone poles; most buildings destroyed, except for concrete reinforced shear wall buildings; *platting* of cars and trucks pressed inwards [2].
12	30–35	Near-complete destruction of houses [2].
13	30	Cladding of light industrial buildings ruptured. Panelling torn-off [2].
14	20–28	Frameless, self-framing steel panel building demolished; rupture of oil storage tanks [2].
15	24	Personnel injuries of a serious nature or possible death are likely from fragments, debris, firebrands or other objects. There is a 10% chance of eardrum rupture [7].
16	15–20	Unreinforced concrete or cinderblock walls shattered [2].
17	20	Heavy machines in industrial buildings suffer little damage; steel frame building distorted and pulled away from foundations [2].
18	18	Lower limit of serious structural damage; 50% destruction of brickwork of houses [2].
19	16	Personnel may suffer temporary hearing loss or injury from secondary blast effects such as building debris and the tertiary effect of displacement. No fatalities or serious injuries from direct blast are expected [7].
20	15	Partial collapse of walls and roofs of houses [2].

Table 1: Continued.

21	7–15	Corrugated asbestos shattered. Corrugated steel or aluminum panels fastenings fail, followed by buckling; wood panel fastenings fail, panels blown in [2].
22	10	Steel frame of clad buildings slightly distorted [2].
23	5.9–8.3	Personnel are provided a high degree of protection from death or serious injury with injuries that do occur being principally caused by glass breakage and building debris [1].
24	8	Partial demolition of houses, made uninhabitable [2].
25	7	Collapse of roof of a tank [2].
26	3.5–7	Windows usually shattered; occasional damage to window frames [2].
27	5	Minor damage to house structures [2].
28	3	Limited minor structural damage [2].
29	2	Probability of 0.95 of no serious damage beyond this value; some damage to house ceilings; 50% of window glass broken [2].
30	1	Typical threshold for glass breakage [2].
31	0.7	Breakage of small windows under strain [2].
32	0.3	Loud noise similar to sonic boom; occasional glass failure [2].
33	0.2	No structural damage; occasional breaking of large window panes already under strain [2].
34	0.15	Annoying noise [2].

GASEOUS HYDROGEN STORAGE – EXPLOSION HAZARDS

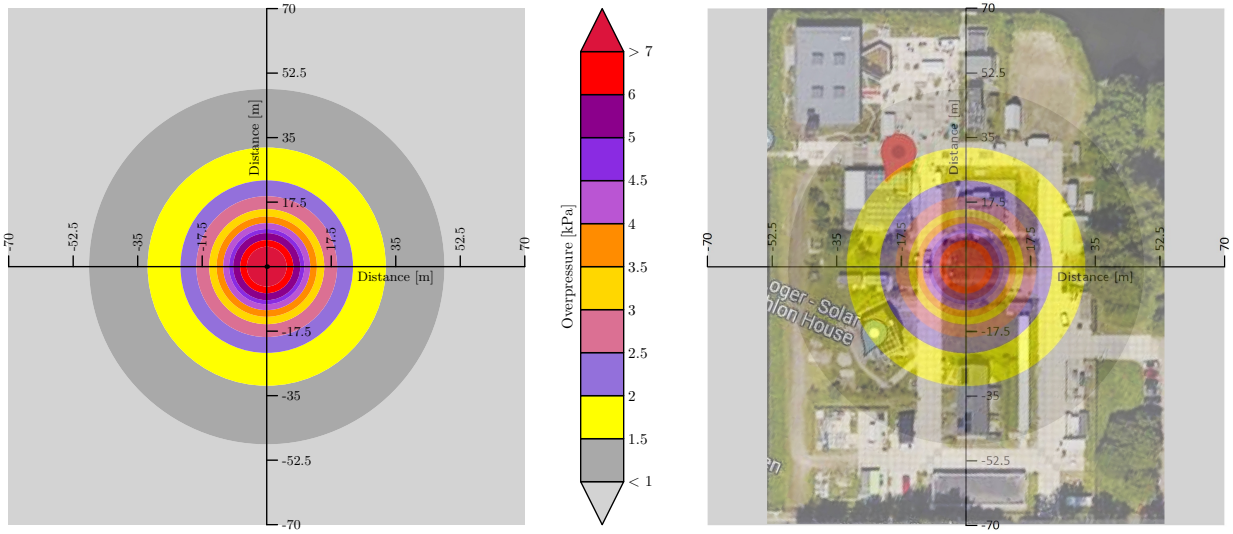


Kjorbo, Norway
Monday 10 June 2019 at 17:30 h
Hydrogen Explosion (3.0 – 3.5 kg H_2)
Glass damage at 60 – 70 m distance
Office at 60 m distance
Houses at $>$ 225 m distance

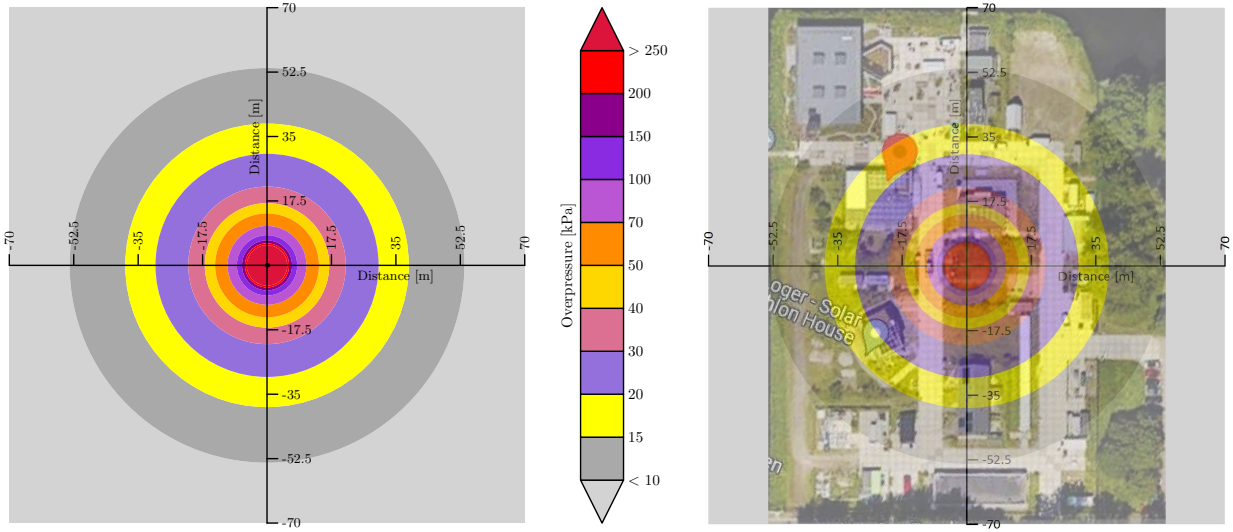


DELFT UNIVERSITY OF TECHNOLOGY – GREEN VILLAGE

Explosion involving 3.5 kg hydrogen Blast calculation according to Ref. [8].

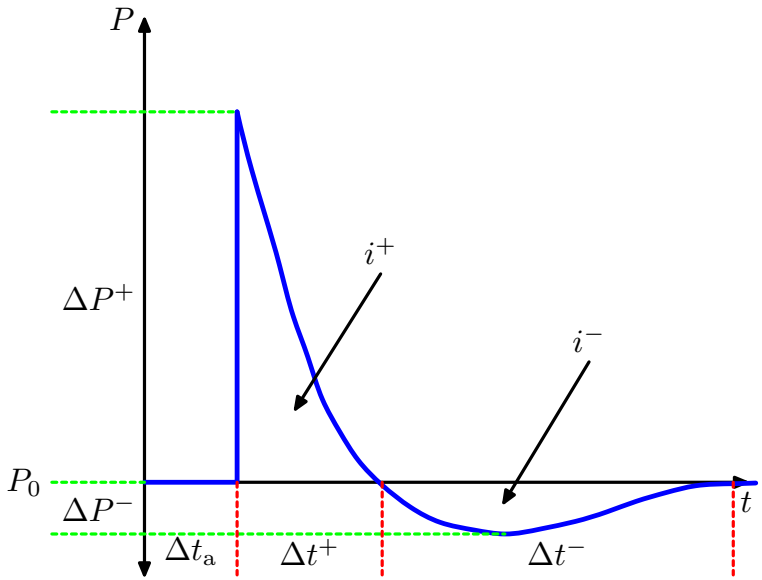


Deflagration

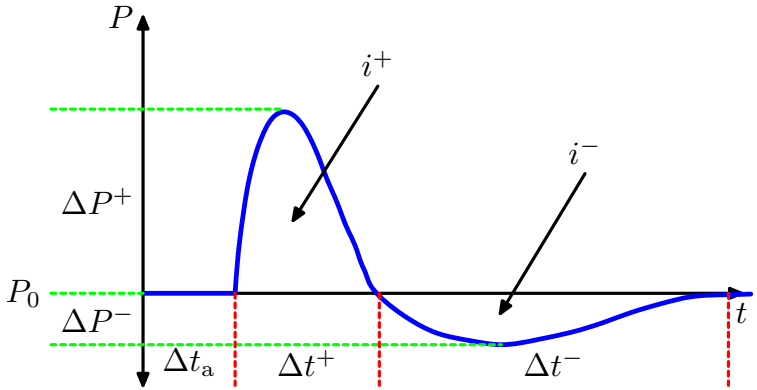


Detonation

PRESSURE WAVEFORM – BLAST DOMAIN AND ACOUSTIC DOMAIN



Blast Domain

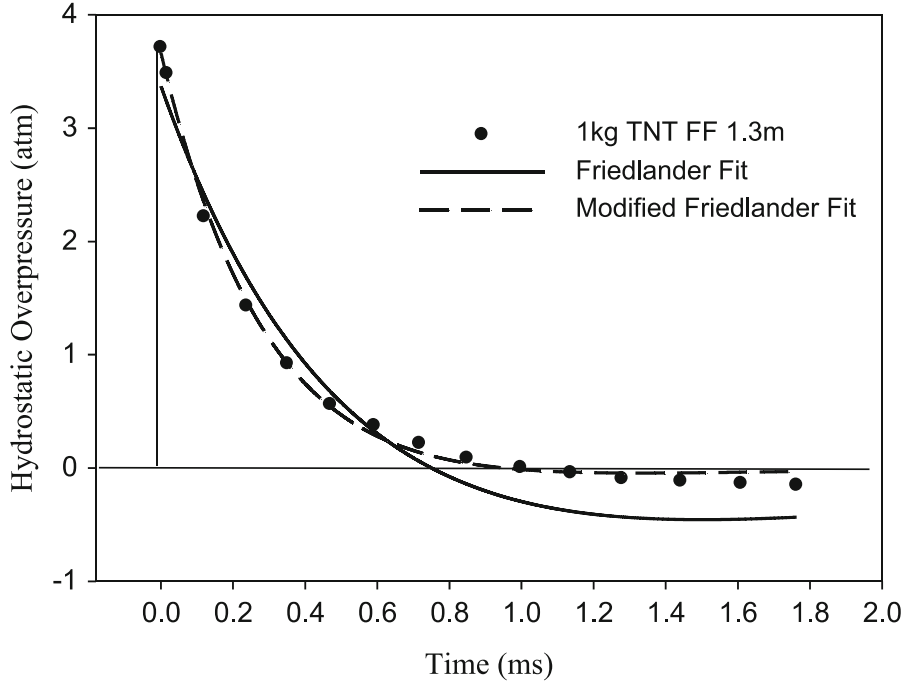


Acoustic Domain

ΔP^+: Peak overpressure
ΔP^-: Peak under pressure
i^+: Positive phase impulse $\int_{\Delta t^+} |P(t) - P_0|\, dt$
i^-: Negative phase impulse $\int_{\Delta t^-} |P(t) - P_0|\, dt$

Δt_a: Arrival time
Δt^+: Positive phase duration
Δt^-: Negative phase duration

PRESSURE WAVEFORM – PARAMETRIZATION



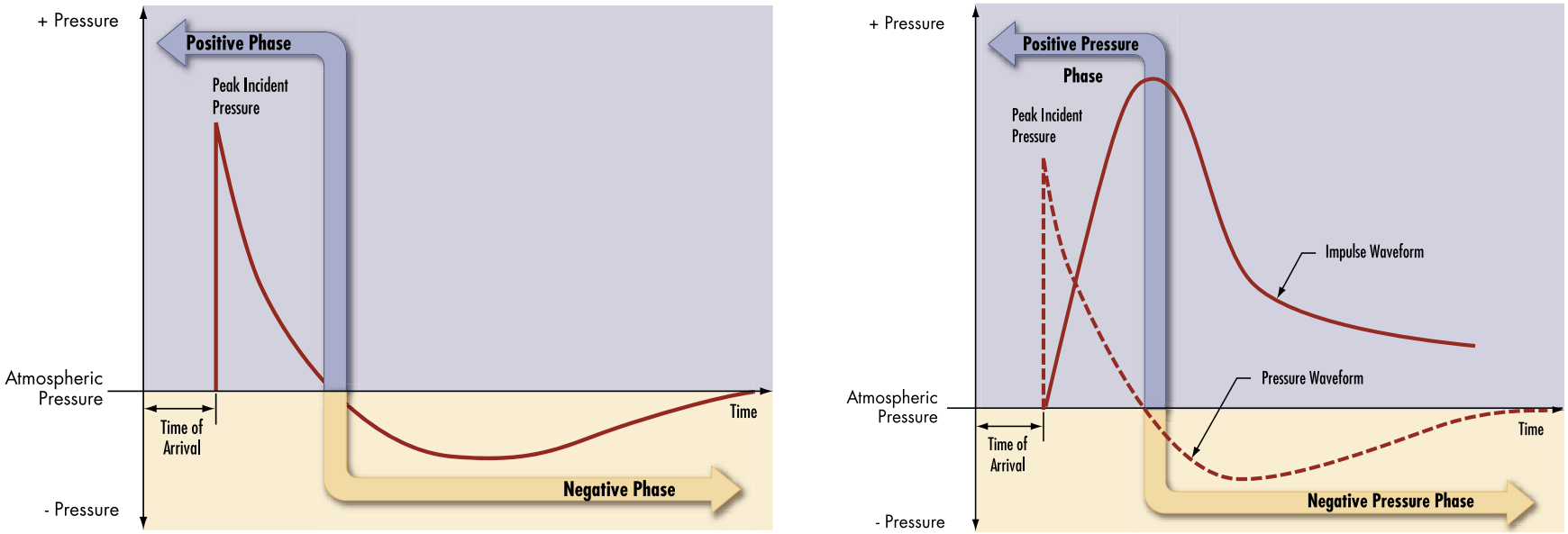
Air blast at 1.3 m from a free-field 1 kg TNT explosion [9].

Friedlander Equation [9]:

$$\Delta P = \Delta P^{+} \left[1 - \frac{\Delta t}{\Delta t^{+}}\right] \exp\left[-\frac{\Delta t}{\Delta t^{+}}\right]$$

Modified Friedlander Equation [9]:

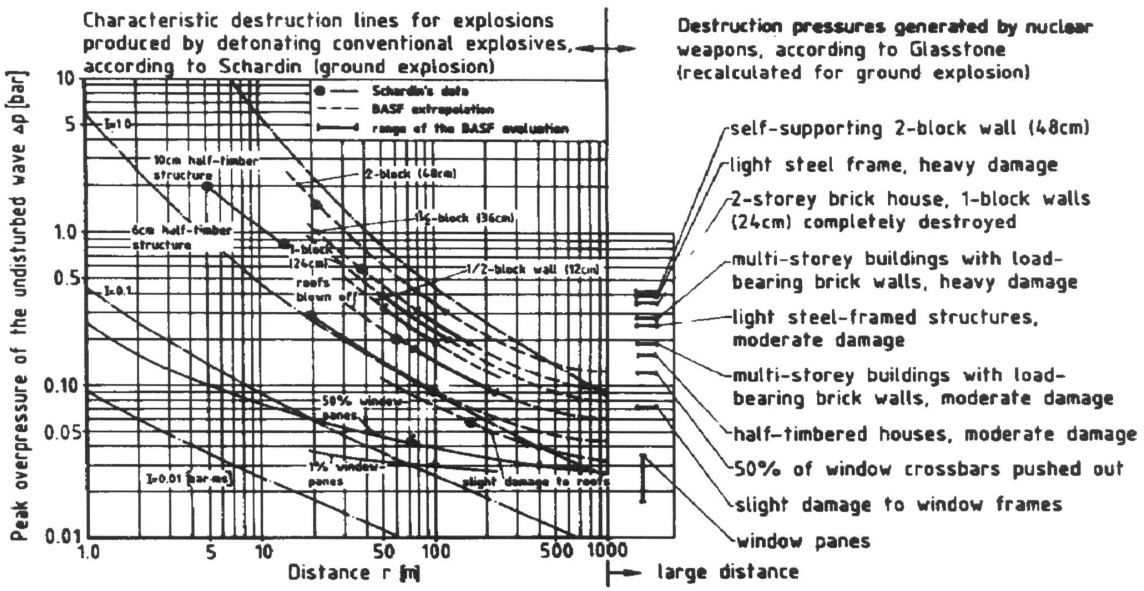
$$\Delta P = \Delta P^{+} \left[1 - \frac{\Delta t}{\Delta t^{+}}\right] \exp\left[-\alpha\frac{\Delta t}{\Delta t^{+}}\right]$$



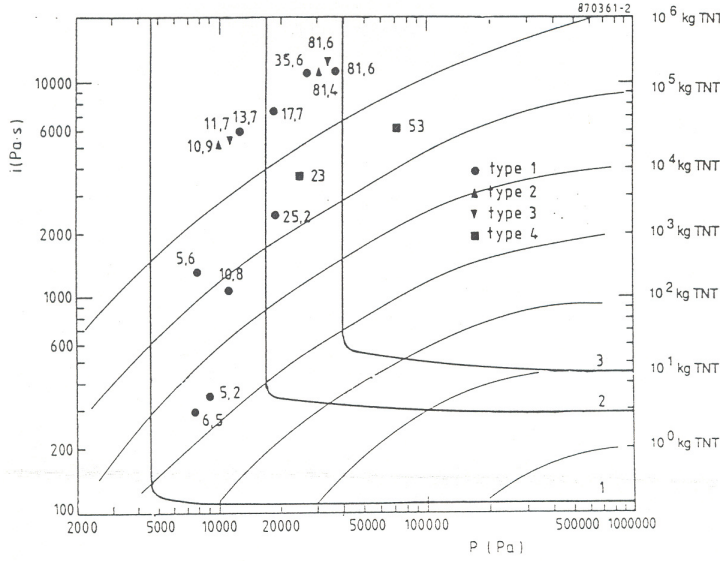
Pressure waveform, $P(t)$, and impulse waveform, $\int |P(t) - P_0|\, dt$, generated by a detonation [4].

Pressure waveform $= P(t)$

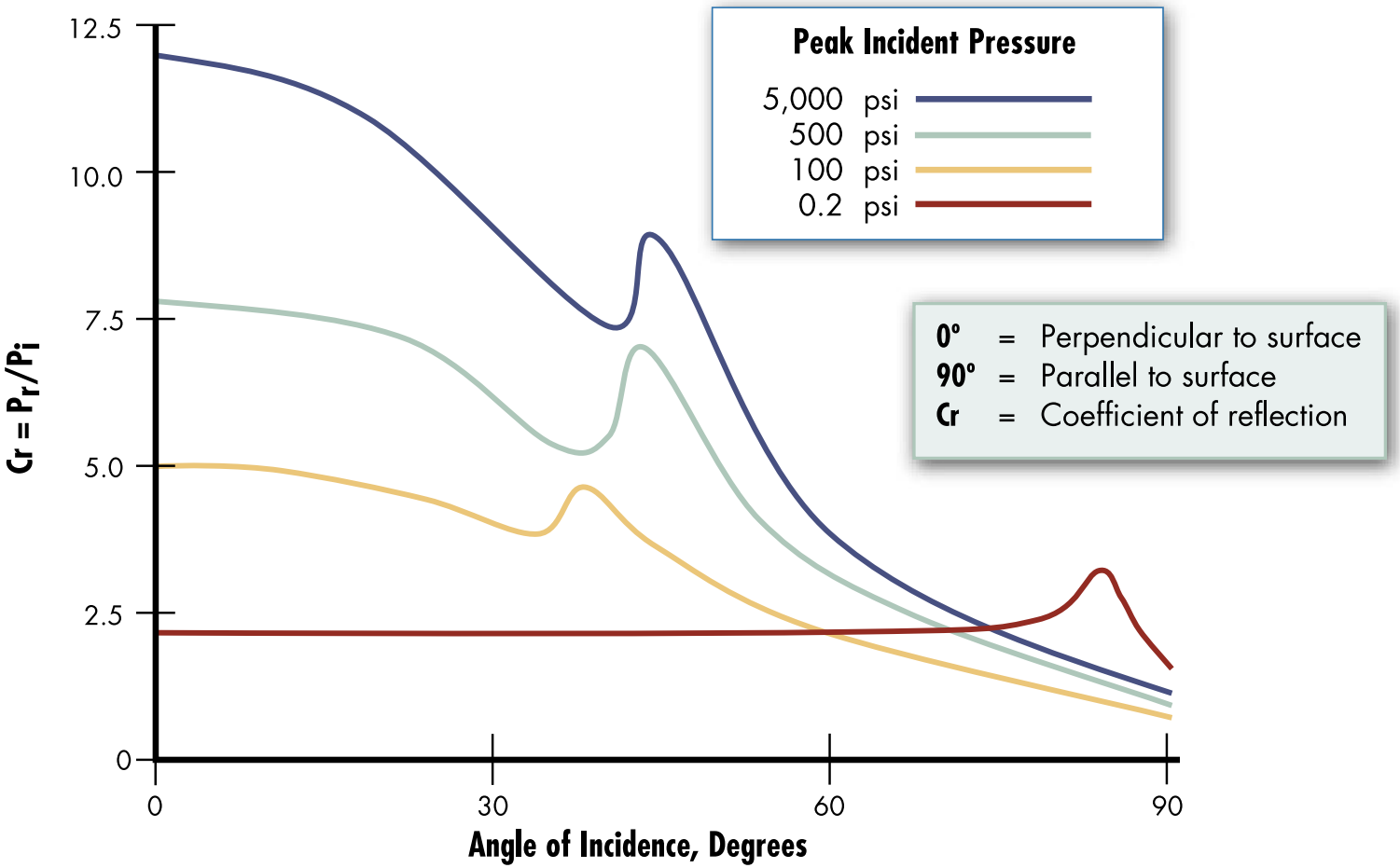
Impulse waveform $= \int |P(t) - P_0|\, dt \quad \Longrightarrow \quad i^+ = \int_{\Delta t^+} |P(t) - P_0|\, dt \qquad i^- = \int_{\Delta t^-} |P(t) - P_0|\, dt$



Schardin destruction curves



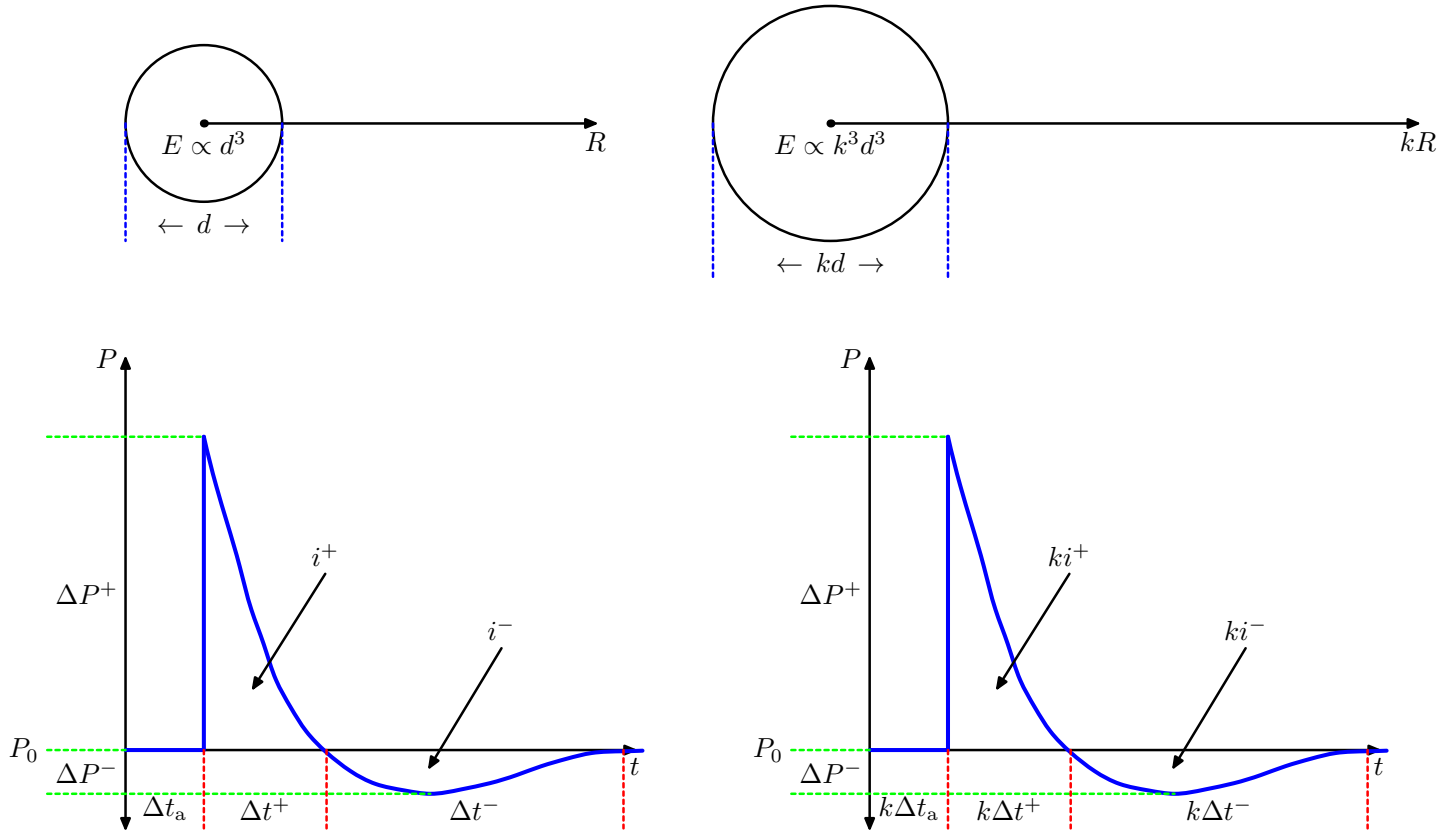
Pressure impulse diagram



Reflected pressure coefficient versus angle of incidence [4].

Acoustic impedance: $z = \rho c$. Reflection coefficient: $\Gamma = \dfrac{z_{\mathrm{s}} - z_{\mathrm{g}}}{z_{\mathrm{s}} + z_{\mathrm{g}}}$.

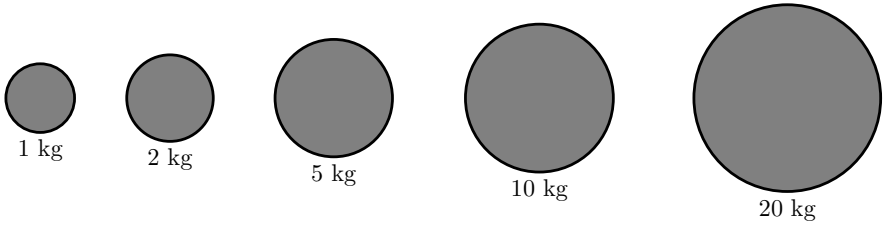
BLAST SCALING



Blast scaling: $\overline{R} = \dfrac{R}{(E/P_0)^{1/3}}$ $\overline{\Delta P^+} = \dfrac{P^+ - P_0}{P_0}$ $\overline{\Delta P^-} = \dfrac{P^- - P_0}{P_0}$

$\overline{i^+} = \dfrac{i^+ a_0}{\left(EP_0^2\right)^{1/3}}$ $\overline{i^-} = \dfrac{i^- a_0}{\left(EP_0^2\right)^{1/3}}$ $\overline{\Delta t^+} = \dfrac{\Delta t^+ a_0}{(E/P_0)^{1/3}}$ $\overline{\Delta t^-} = \dfrac{\Delta t^- a_0}{(E/P_0)^{1/3}}$ $\overline{\Delta t_\mathrm{a}} = \dfrac{\Delta t_\mathrm{a} a_0}{(E/P_0)^{1/3}}$

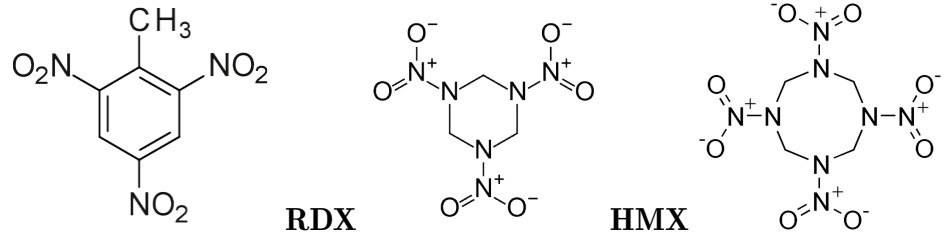
HOPKINSON – CRANZ SCALING

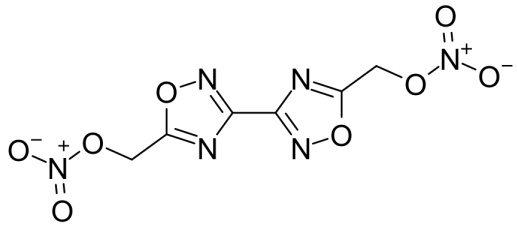


$$\boxed{\Delta P^+ = \beta M^{1/3} = \beta \sqrt[3]{M}}$$

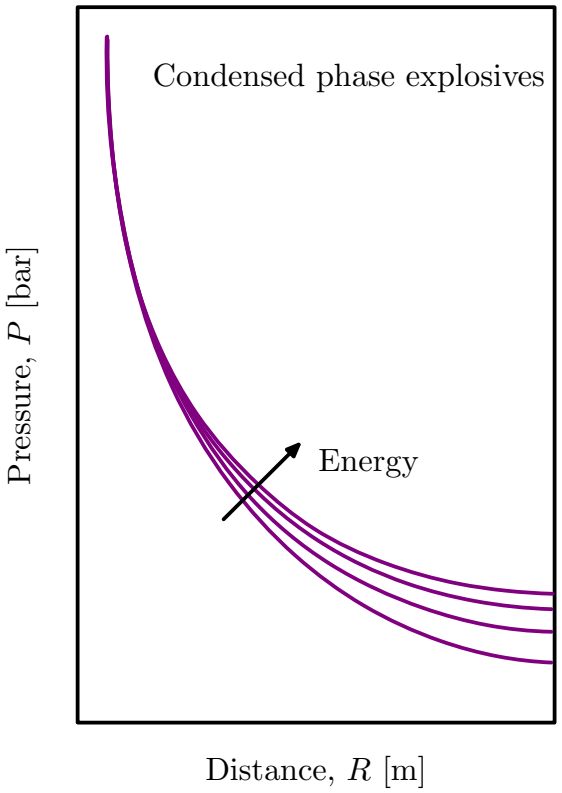
$$\mathrm{E} \propto M \Longrightarrow \boxed{\Delta P^+ = \tilde{\beta} E^{1/3}}$$

$$\Longrightarrow \quad \beta = \frac{\Delta P^+}{M^{1/3}} \text{ and } \tilde{\beta} = \frac{\Delta P^+}{E^{1/3}}$$

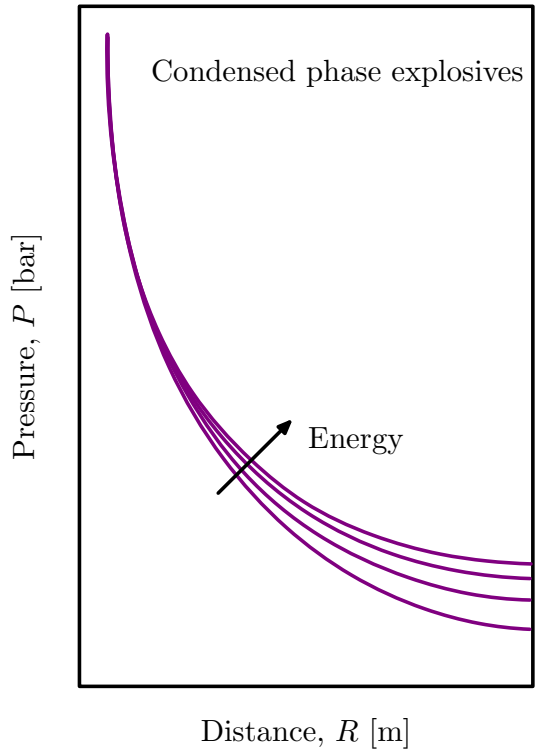


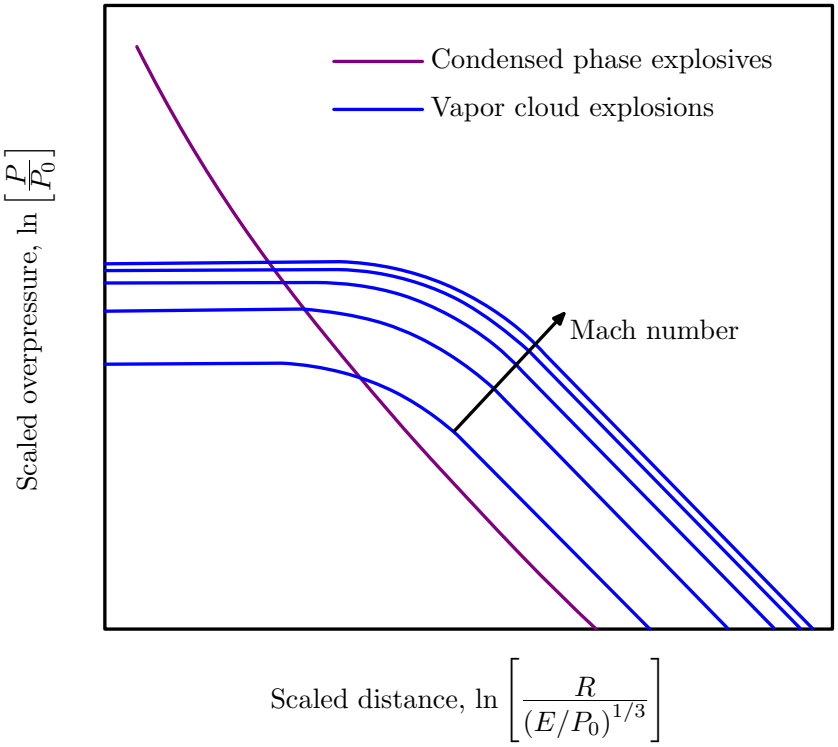


Substance	**TNT**	**RDX**	**HMX**	**Bis-oxadiazole**	**H_2**
Energy release [MJ kg^{-1}]:	4.68	5.15	5.85	7.02	142
Detonation pressure [bar]:	$2.05{\cdot}10^5$	$3.30{\cdot}10^5$	$4.00{\cdot}10^5$	$2.94{\cdot}10^5$	14.5
Detonation velocity [km s^{-1}]:	6.95	8.75	9.10	8.180	1.968
TNT-equivalency [-]:	1.1	1.2	1.4	1.68	34



SACH SCALING





Sach variables: $\overline{R} = \dfrac{R}{(E/P_0)^{1/3}}$ $\overline{P} = \dfrac{P}{P_0}$ $\overline{i} = \dfrac{ia_0}{\left(EP_0^2\right)^{1/3}}$

Parametrization scaled blast curve: $\ln \overline{P} = \alpha_1 \left[\dfrac{1}{\ln \overline{P}}\right] + \alpha_2 \left[\dfrac{1}{\ln \overline{P}}\right]^2 + \alpha_3 \left[\dfrac{1}{\ln \overline{P}}\right]^3 + \ldots$

TNT EQUIVALENCY METHOD

For vapor cloud explosions, the equivalent mass of TNT is calculated using the following expression:

$$M_{\mathrm{TNT}} = \eta \frac{M\,\Delta H_{\mathrm{c}}}{\Delta H_{\mathrm{TNT}}} \quad \text{or} \quad M_{\mathrm{TNT}} = \eta \frac{M\,\Delta H_{\mathrm{d}}}{\Delta H_{\mathrm{TNT}}} \tag{1}$$

where:
M is the mass (kg) of fuel in the cloud or a quantity of condensed phase explosives
ΔH_{c} is the lower heat of combustion of the fuel ($\mathrm{kJ\,kg^{-1}}$)
ΔH_{d} is the decomposition energy release by a condensed phase explosive ($\mathrm{kJ\,kg^{-1}}$)
η is the explosion yield factor (-)
ΔH_{TNT} is the decomposition energy of TNT (4680 $\mathrm{kJ\,kg^{-1}}$)
M_{TNT} the mass of TNT that would produce the same degree of damage (kg)

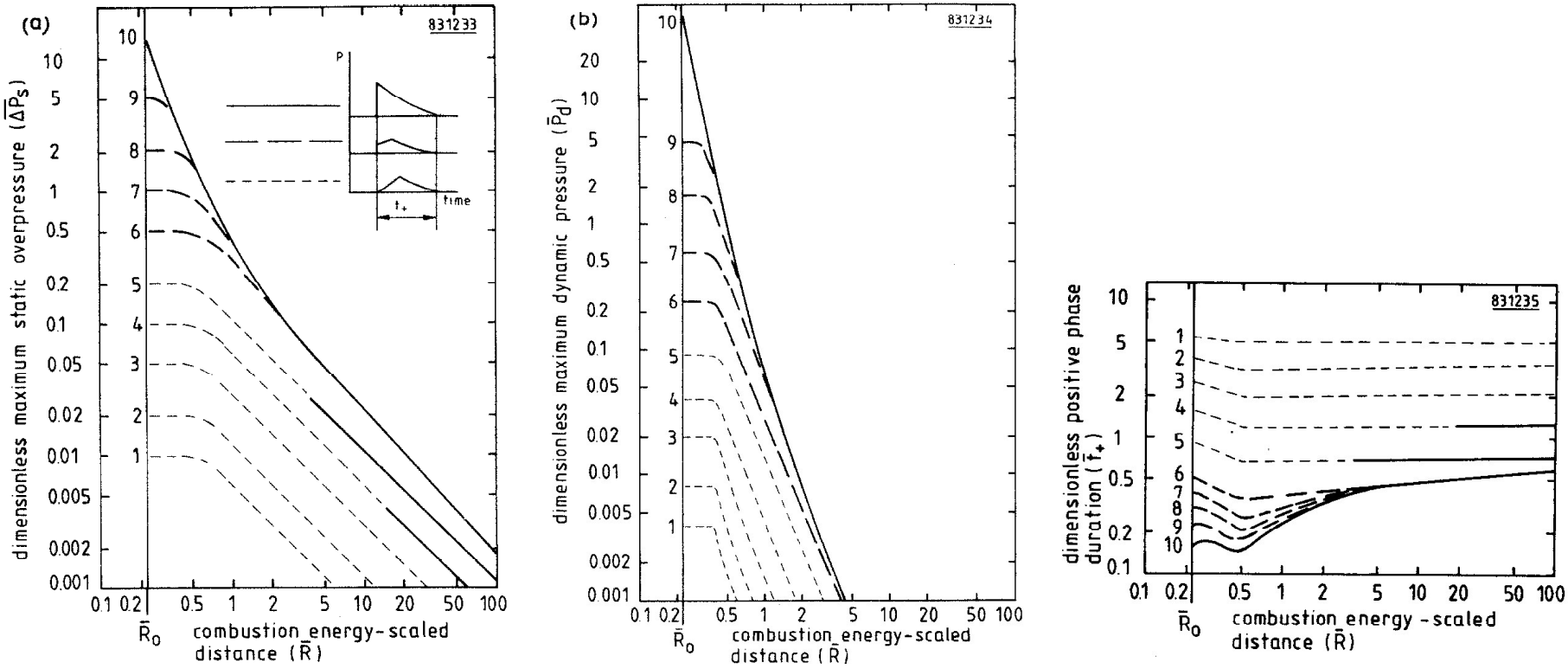
Although the value of η is influenced by the reactivity of the fuel involved and the eventual partial confinement of the cloud, the currently accepted value is 3% ($\eta = 0.03$) for hydrocarbons. Whereas a value of 10% ($\eta = 0.1$) is being applied for hydrogen.

Definition of a TNT*-equivalent:

$\boxed{1\ \mathrm{kT\ TNT^*} = 10^{12}\ \mathrm{cal} = 4.18{\cdot}10^{12}\ \mathrm{J}}$ or, equally $\boxed{1\ \mathrm{kg\ TNT^*} = 10^{6}\ \mathrm{cal} = 4.18{\cdot}10^{6}\ \mathrm{J}}$

Notice that the chemical substance TNT has a TNT*-equivalency of ($4.68\ \mathrm{MJ\,kg^{-1}}/4.18\ \mathrm{MJ\,kg^{-1}}$) = 1.12

MULTI ENERGY METHOD – NOMOGRAMS



• Van den Berg A.C. The multi-energy method - a framework for vapor cloud explosion blast prediction. *Journal of Hazardous Materials*, 12:1–10, 1985 [11].

• Van den Berg A.C. A 1-D variable flame speed blast simulation code using a flux-corrected transport algorithm. Report PML 1980-162, TNO Prins Maurits Laboratory, The Netherlands, 1980 [16].

• Wiekema B.J. Vapour cloud explosion model. *Journal of Hazardous Materials*, 3:221–232, 1971 [17].

MULTI ENERGY METHOD – BLAST STRENGTH INDEX

Selection of the Blast Strength Index							
Ignition energy		Level of obstruction			Degree of confinement		Blast strength
Weak	Strong	Weak	Strong	Not Established	Established	Not Established	
	X	X			X		7 – 10
	X	X				X	7 – 10
X		X			X		5 – 7
	X		X		X		5 – 7
	X		X			X	4 – 6
	X			X	X		4 – 6
X		X				X	4 – 5
	X			X		X	4 – 5
X			X		X		3 – 5
X			X			X	2 – 3
X				X	X		1 – 2
X				X		X	1

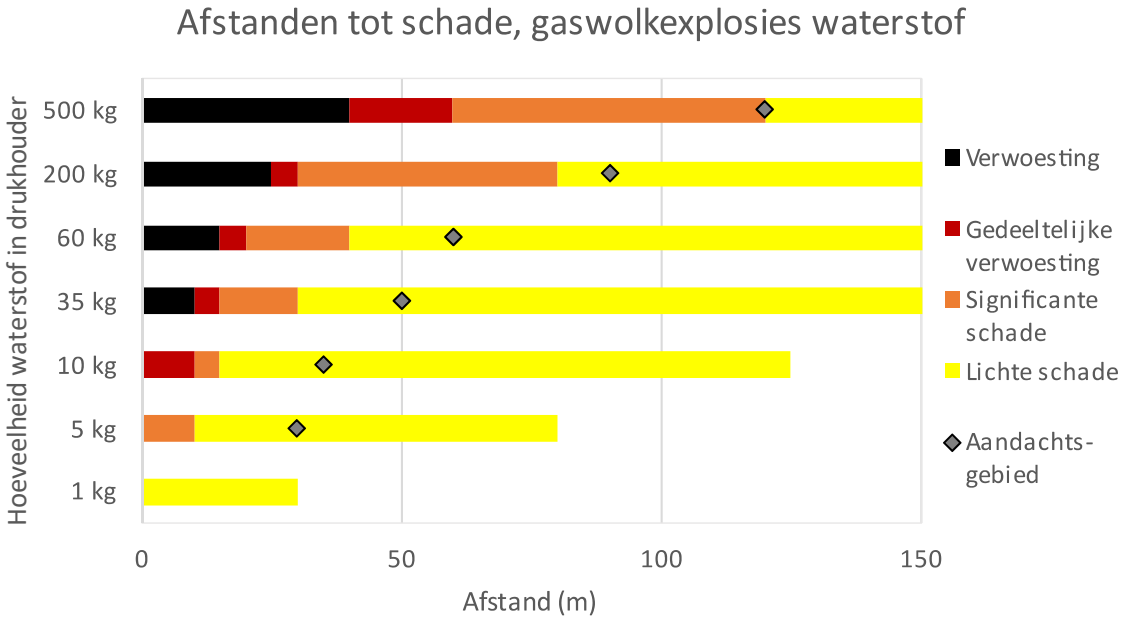
Source:

• Kinsella K.G. A rapid assessment methodology for the prediction of vapour cloud explosions. Research Report 357, Technical Research Centre of Finland, 1993 [18].

MULTI ENERGY METHOD – SAFETY DISTANCES

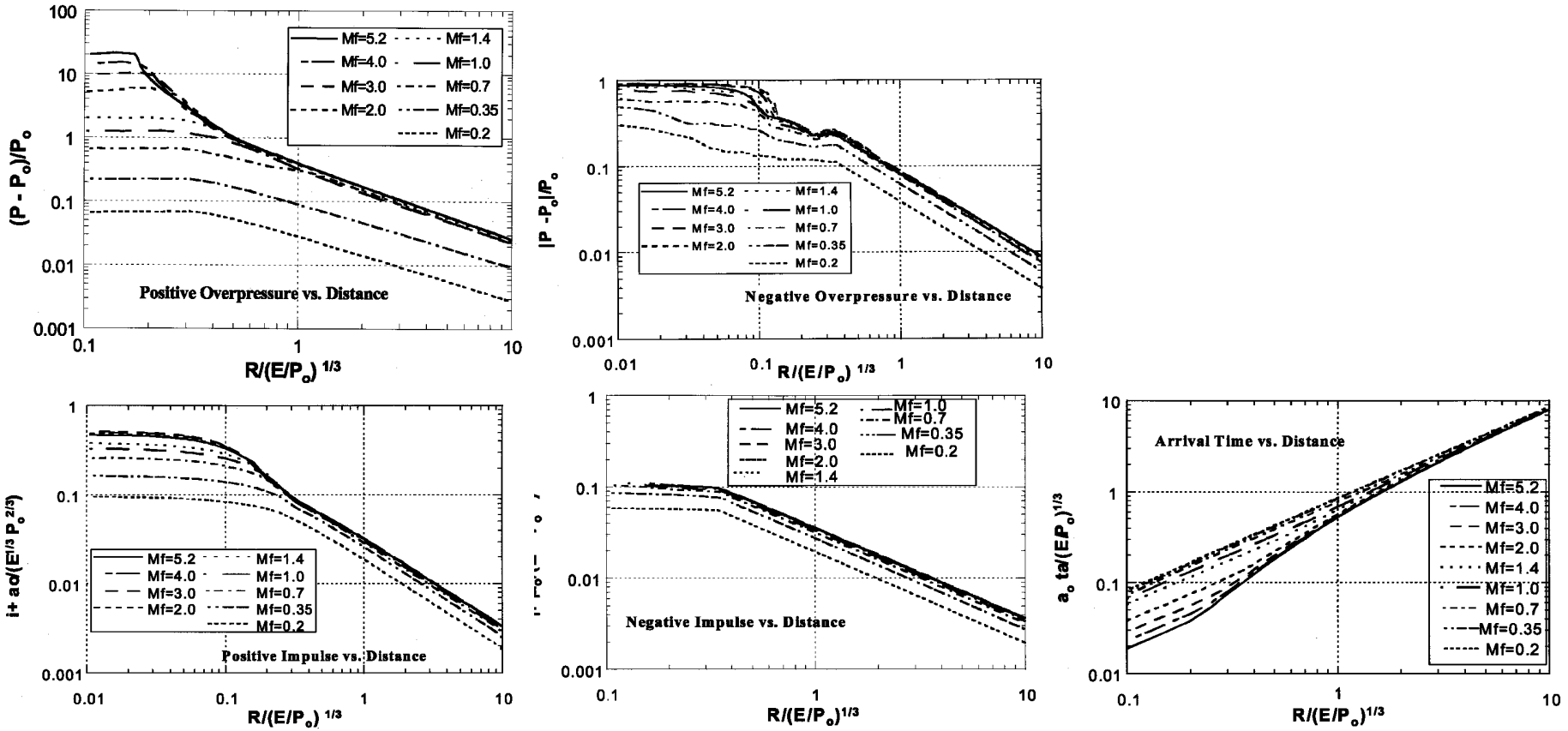
Soort schade	Overdruk (bar)	Impuls (Pa·s)
Lichte schade, ondergrens voor effecten (voor overdruk: ondergrens ruitbreuk dubbelglas [5]; voor impuls: 50% ruitbreuk van grote ruiten [6])	0,02	20
Significante schade (voor overdruk: begrenzing van aandachtsgebied, 2,5% letaliteit [7], 100% ruitbreuk [5]; voor impuls: lichte, herstelbare schade aan constructies [5])	0,1	200
Gedeeltelijke verwoesting (50-75% van muren bezwijken) (zie opmerking)	0,3	550
Verwoesting van gebouwen (zie opmerking)	0,6	850

Source: Van der Linden M. and Wolting A.G. Effecten van waterstofexplosies. Public report 2024-0032, National Institute for Public Health and the Environment (RIVM), The Netherlands, 2024 [19].



Results obtained with:
Blast Strength Index = 10

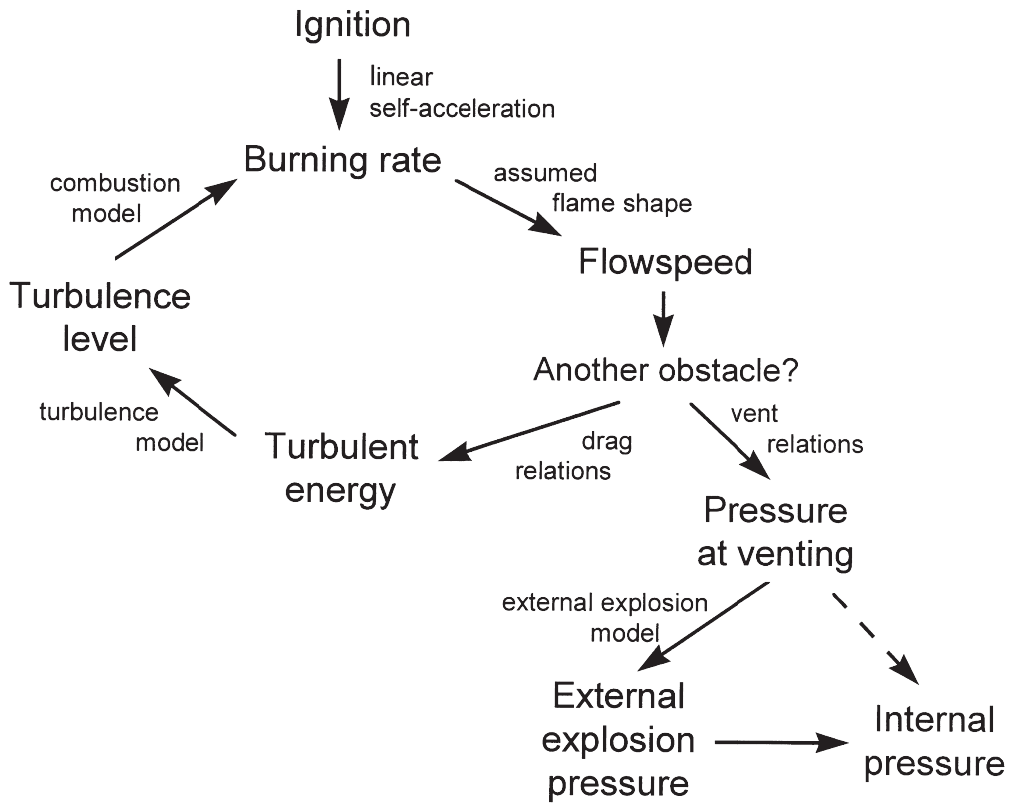
BAKER-STREHLOW-TANG METHOD – NOMOGRAMS

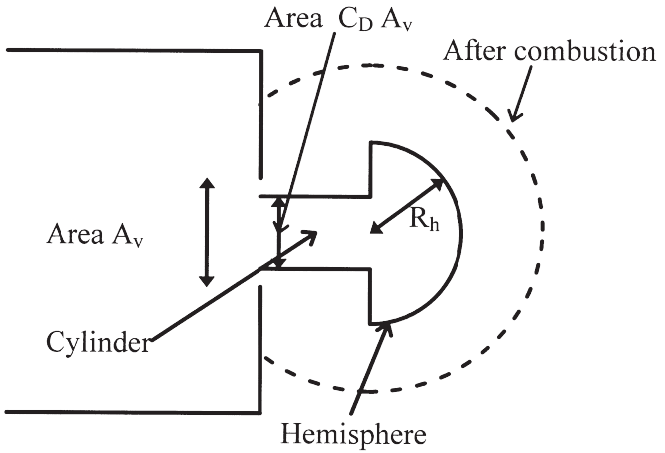


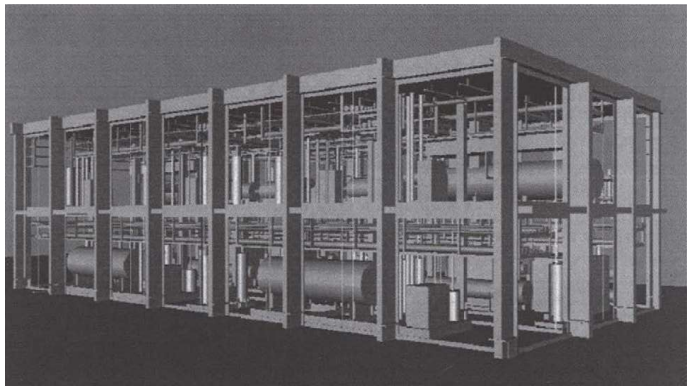
• Tang M.J. and Baker Q.A. A new set of blast curves from vapor cloud explosion. *Process Safety Progress*, 18:235–240, 1999 [8].

• Baker Q.A., Tang M.J., Scheier E.A. and Silva G.J. Vapor cloud explosion analysis. *Process Safety Progress*, 15:106–109, 1996 [20].

SCOPE & CONGESTION ASSESSMENT METHOD







Source: Refs. [13, 14].

SHELL FRED CODE & DOROFEEV MODEL

Source: Dorofeev S.B. Evaluation of safety distances related to unconfined hydrogen explosions. *International Journal of Hydrogen Energy*, 32:2118–2124, 2007 [15].

$$S_{\mathrm{f}} = \sigma S_{u\mathrm{T}} \left[1 + \frac{4}{3} \frac{\sigma y}{x} \frac{R^{\alpha}}{(\sigma x)^2} \right] \tag{2}$$

$$\frac{S_{u\mathrm{T}}}{S_{u\mathrm{L}}} = a \left(\frac{v'_{\mathrm{rms}}}{S_{u\mathrm{T}}} \right)^{1/2} \left(\frac{\ell_t}{\delta_{\mathrm{L}}} \right)^{1/6} \tag{3}$$

$$v'_{\mathrm{rms}} = b\, S_{\mathrm{f}} \frac{\sigma - 1}{\sigma} \tag{4}$$

Combination of (2), (3) and (4):

$$S_{\mathrm{f}} = a^2 \sigma (\sigma - 1) S_{u\mathrm{L}} \left[1 + \frac{4}{3} \frac{\sigma y}{x} \frac{R^{\alpha}}{(\sigma x)^2} \right]^2 \left(\frac{\ell_t}{\delta_{\mathrm{L}}} \right)^{1/3} \tag{5}$$

FORMATION OF A BLAST WAVE BY A VERY INTENSE EXPLOSION

The air wave surrounding an expanding sphere

By G. I. Taylor, F.R.S.

(*Received* 5 *December* 1939)

[For summary see p. 292.]

Introduction

When the surface of a sphere vibrates in any assigned manner the spherical sound waves which are propagated outwards can be represented by well-known formulae provided that the motion is such that only small changes in air density occur. When the motion of the spherical surface is radial the

Source: Taylor G.I. The air wave surrounding an expanding sphere. *Proceedings of the Royal Society of London, Series A: mMathematical and Physical Sciences*, 186:273–292, 1946 [21].

The formation of a blast wave by a very intense explosion
I. Theoretical discussion

By Sir Geoffrey Taylor, F.R.S.

(*Received* 6 *October* 1949)

Summary and introduction

This paper was written early in 1941 and circulated to the Civil Defence Research Committee of the Ministry of Home Security in June of that year. The present writer had been told that it might be possible to produce a bomb in which a very large amount of energy would be released by nuclear fission—the name atomic bomb had not then been used—and the work here described represents his first attempt to form

Source: Taylor G.I. The formation of a blast wave by a very intense explosion. I. Theoretical discussion. *Proceedings of the Royal Society of London, Series A: Mathematical and Physical Sciences*, 201:159–174, 1950 [22].

The formation of a blast wave by a very intense explosion.
II. The atomic explosion of 1945

By Sir Geoffrey Taylor, F.R.S.

(*Received* 10 *November* 1949)

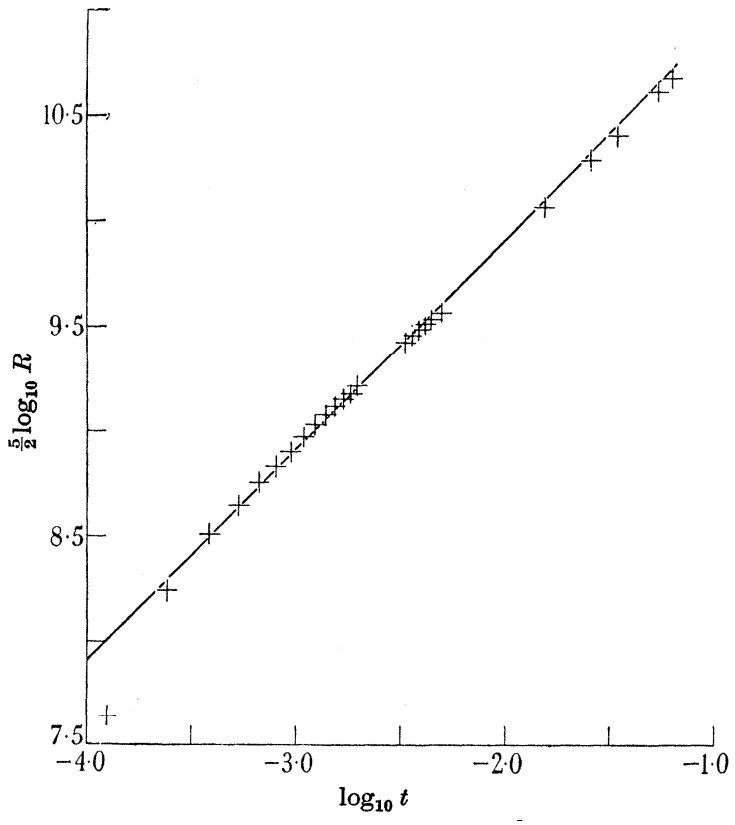
[Plates 7 to 9]

Photographs by J. E. Mack of the first atomic explosion in New Mexico were measured, and the radius, R, of the luminous globe or 'ball of fire' which spread out from the centre was determined for a large range of values of t, the time measured from the start of the explosion. The relationship predicted in part I, namely, that $R^{\frac{5}{2}}$ would be proportional to t, is surprisingly accurately verified over a range from $R = 20$ to 185 m. The value of $R^{\frac{5}{2}}t^{-1}$ so found was used

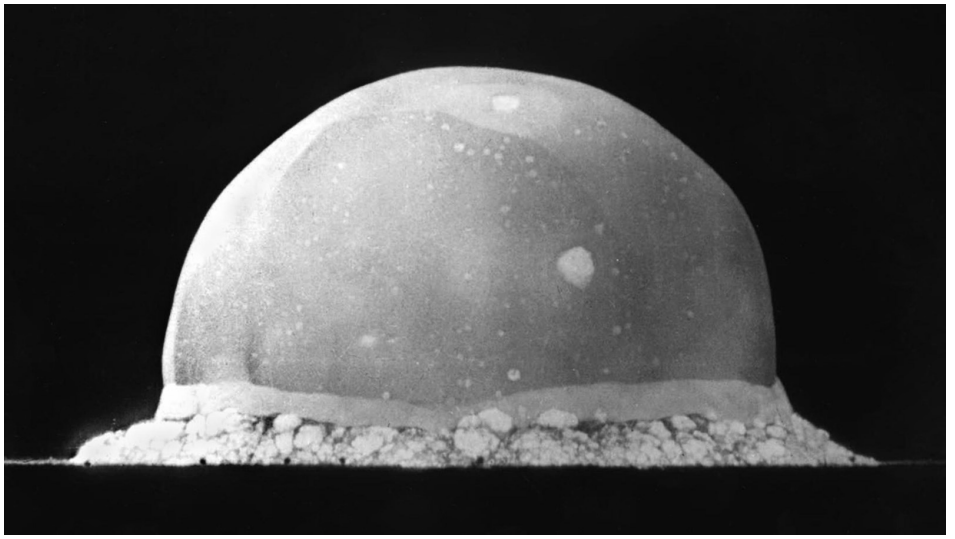
Source: Taylor G.I. The formation of a blast wave by a very intense explosion. II. The atomic explosion of 1945. *Proceedings of the Royal Society of London, Series A: Mathematical and Physical Sciences*, 201:175–186, 1950 [23].

FORMATION OF A BLAST WAVE BY A VERY INTENSE EXPLOSION

$$\boxed{R = C(\gamma)E^{1/5}\rho_0^{-1/5}t^{2/5}}$$ where $$C(\gamma) = \frac{\gamma - 1 + (\gamma+1)y_1}{\gamma+1+(\gamma-1)y_1}\frac{\gamma-1}{\gamma+1}$$ and $$\gamma = C_P/C_V$$



y_1 (atm.)	r/r_0	ρ_1/ρ_0 uncorrected	C	ρ_1/ρ_0 corrected	R/r_0
10	(0·360)	1·155	0·753	0·873	0·249
20	0·337	0·704	0·858	0·605	0·198
30	0·325	0·527	0·900	0·475	0·173
40	0·316	0·430	0·923	0·397	0·157
60	0·304	0·321	0·947	0·305	0·137
100	0·289	0·223	0·968	0·216	0·116
500	0·247	0·071	—	0·071	0·068
5000	0·200	0·013	—	0·013	0·031



Nuclide	Half-life (y)	Critical mass (kg)	Diameter (cm)
uranium-233	159,200	15	11
uranium-235	703,800,000	52	17
neptunium-236	154,000	7	8.7
neptunium-237	2,144,000	60	18
plutonium-238	87.7	9.04–10.07	9.5–9.9
plutonium-239	24,110	10	9.9
plutonium-240	6561	40	15
plutonium-241	14.3	12	10.5
plutonium-242	375,000	75–100	19–21
americium-241	432.2	55–77	20–23
americium-242m	141	9–14	11–13
americium-243	7370	180–280	30–35
curium-243	29.1	7.34–10	10–11
curium-244	18.1	13.5–30	12.4–16
curium-245	8500	9.41–12.3	11–12
curium-246	4760	39–70.1	18–21
curium-247	15,600,000	6.94–7.06	9.9
berkelium-247	1380	75.7	11.8-12.2
berkelium-249	0.9	192	16.1-16.6
californium-249	351	6	9
californium-251	900	5.46	8.5
californium-252	2.6	2.73	6.9
einsteinium-254	0.755	9.89	7.1

PLUTONIUM

Formation:

$$^{1}_{0}\mathrm{n} + {}^{238}_{92}\mathrm{U} \longrightarrow {}^{239}_{92}\mathrm{U}$$

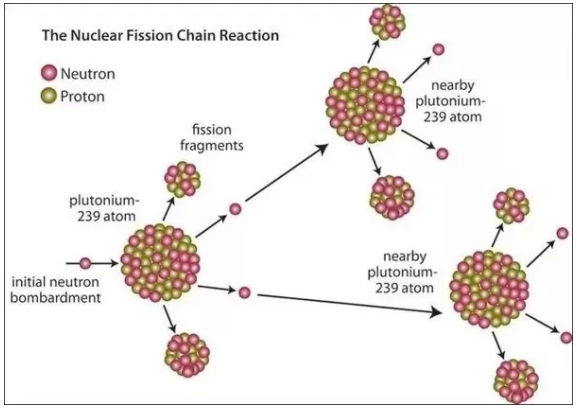
$${}^{239}_{92}\mathrm{U} \xrightarrow[\text{mins}]{23} {}^{239}_{93}\mathrm{Np} + \beta^{-}$$

$${}^{239}_{93}\mathrm{Np} \xrightarrow[\text{days}]{2.36} {}^{239}_{94}\mathrm{Pu} + \beta^{-}$$

Natural decay:

$${}^{239}_{94}\mathrm{Pu} \xrightarrow[\text{years}]{24100} {}^{235}_{92}\mathrm{U} + {}^{4}_{2}\mathrm{He}$$

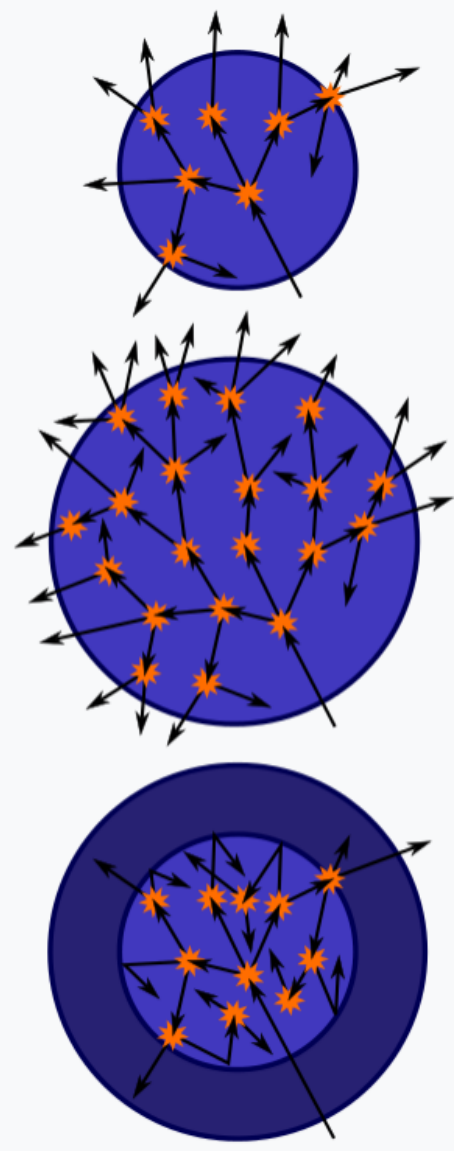
Chain reaction:



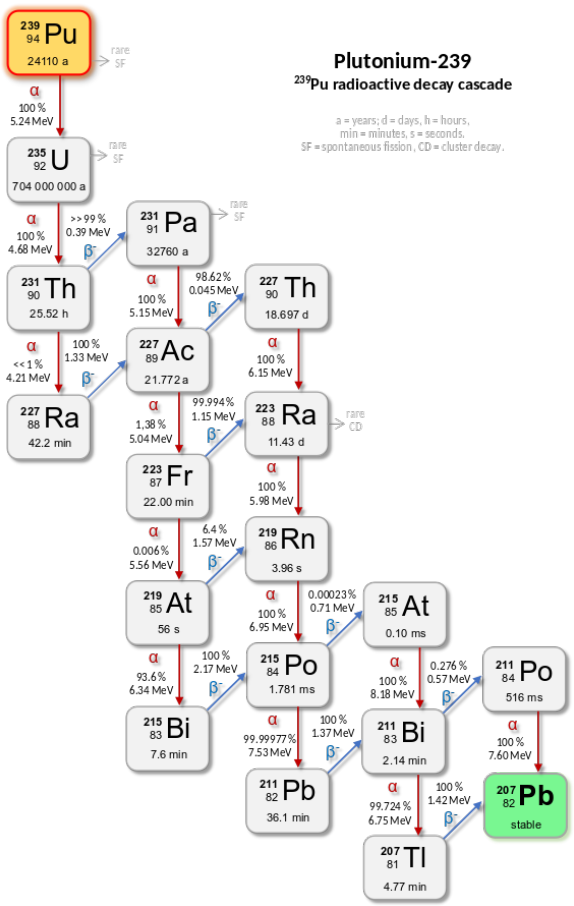
$$^{1}_{0}\mathrm{n} + {}^{239}_{94}\mathrm{Pu} \longrightarrow [{}^{240}_{94}\mathrm{Pu}]$$

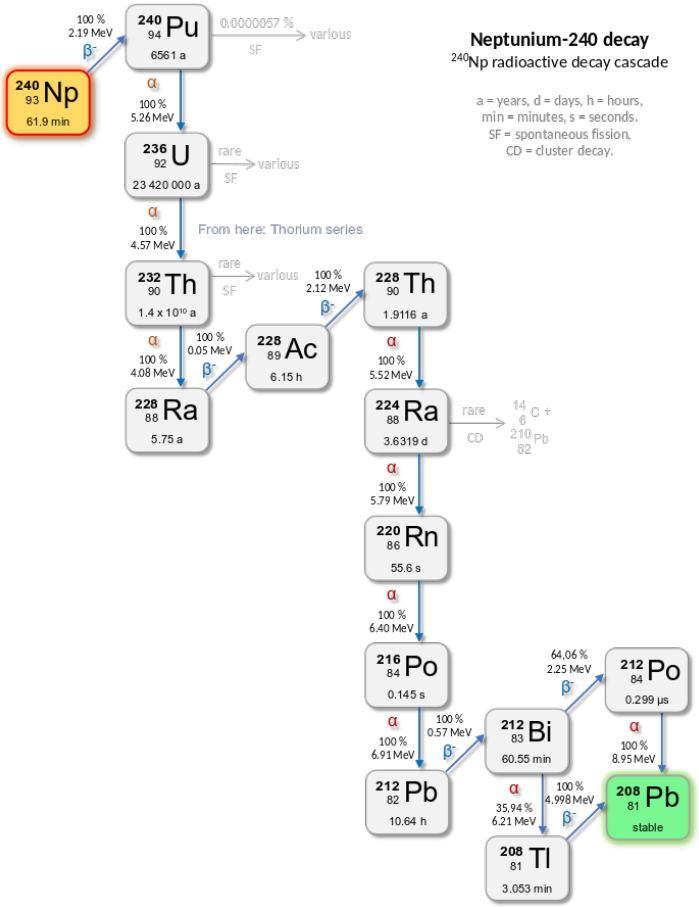
$$[{}^{240}_{94}\mathrm{Pu}] \xrightarrow{73\,\%} {}^{134}_{54}\mathrm{Xe} + {}^{103}_{40}\mathrm{Zr} + 3\,{}^{1}_{0}\mathrm{n}$$

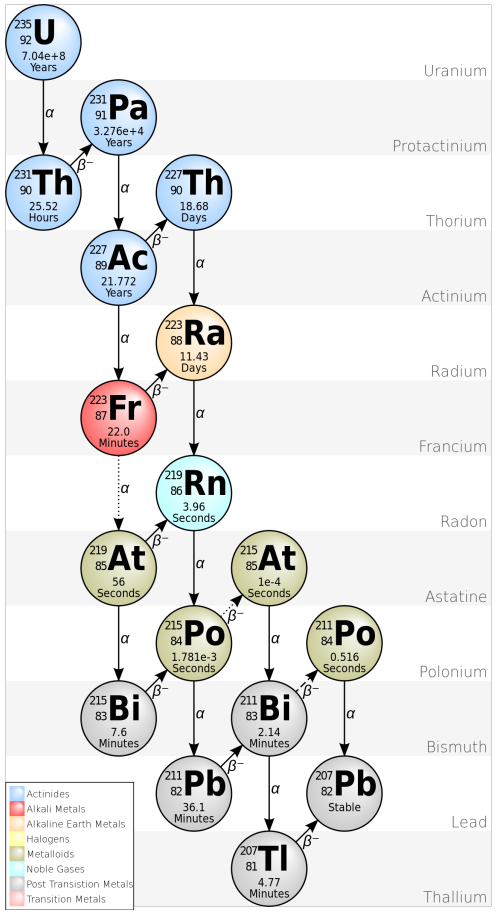
$$[{}^{240}_{94}\mathrm{Pu}] \xrightarrow{27\,\%} {}^{240}_{94}\mathrm{Pu} + \gamma$$



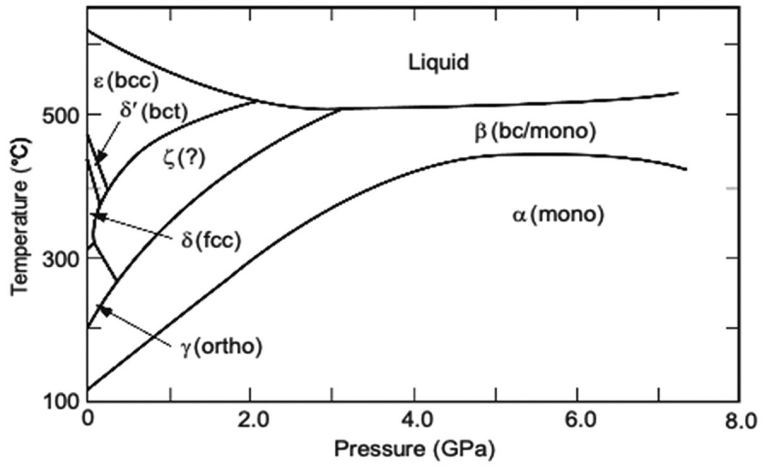
RADIOACTIVE DECAY CASCADE: PLUTONIUM AND URANIUM



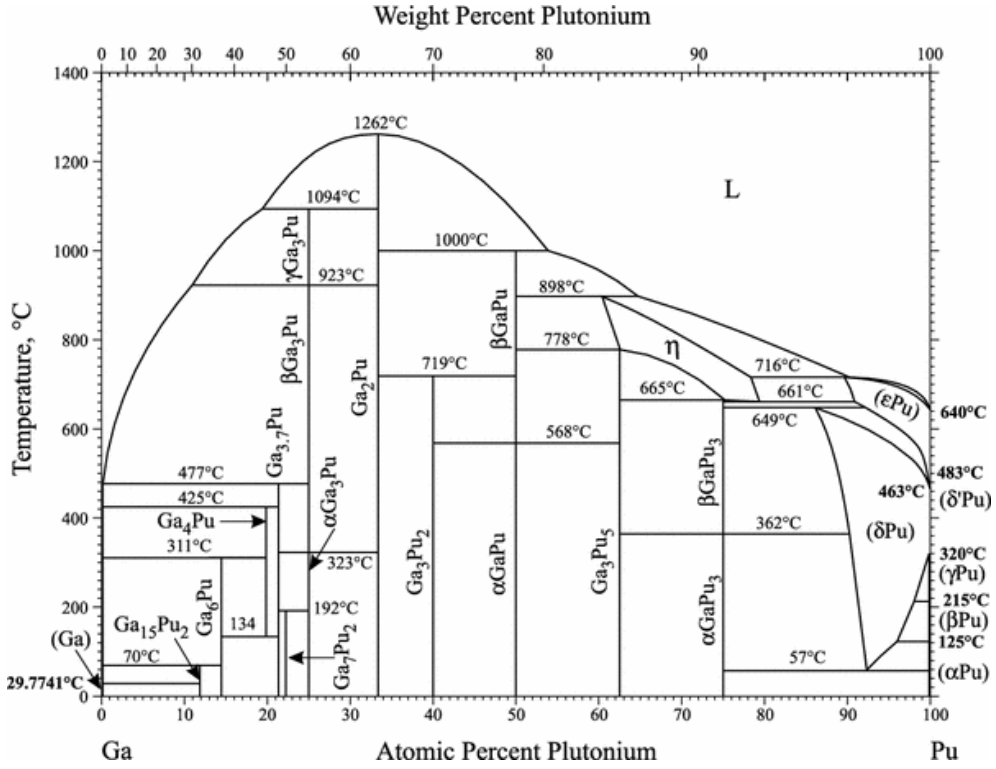




PHASE DIAGRAM: PLUTONIUM AND PLUTONIUM – GALLIUM ALLOY



Plutonium



Plutonium – Gallium Alloy

FORMATION OF A BLAST WAVE BY A VERY INTENSE EXPLOSION

DIMENSIONAL ANALYSIS

Express the shock wave radius R as a power-law function of energy, E, the ambient density, ρ_0, and time t:

$$\begin{aligned} R &= f\left(E, \rho_0, t\right) \\ &= C E^a \rho_0^b \, t^c \end{aligned}$$

Substitute the units of the physical quantities involved,

$$[\mathrm{m}] = \left[\mathrm{kg\,m^2\,s^{-2}}\right]^a \left[\mathrm{kg\,m^{-3}}\right]^b [\mathrm{s}]^c$$

to obtain a system of algebraic equations,

$$\begin{aligned} \mathrm{m}: &\quad 1 = 2a - 3b \\ \mathrm{kg}: &\quad 0 = a + b \\ \mathrm{s}: &\quad 0 = -2a + c \end{aligned}$$

that can be solved to yield:

$$a = 1/5 \qquad b = -1/5 \qquad c = 2/5$$

Hence $\boxed{R = C E^{1/5} \rho_0^{-1/5} t^{2/5}} \quad \Longrightarrow \quad \dfrac{R}{E^{1/5} \rho_0^{-1/5} t^{2/5}} = C$

Bibliography

[1] Ngo T., Mendis P., Gupta A., and Ramsay J. Blast loading and blast effects on structures – An overview. *Electronic Journal of Structural Engineering*, 7:76–91, 2007. Special Issue: Loading on Structures.

[2] Casal J. *Evaluation of the effects and consequences of major accidents in industrial plants*. Industrial Safety Series. Elsevier, Amsterdam, 2008.

[3] Groethe M., Merilo E., Colton J., Chiba S., Sato Y., and Iwabuchi H. Large-scale hydrogen deflagrations and detonations. *International Journal of Hydrogen Energy*, 32:2125–2133, 2007.

[4] Federal Emergency Management Agency (FEMA). *Reference manual to mitigate potential terrorist attacks against buildings*. Number FEMA 426 in Risk Management Series. McGraw-Hill, Washington D.C, December 2003.

[5] Gupta R.K. and Przekwas A. Mathematical models of blast-induced TBI: current status, challenges, and prospects. *Frontiers in Neurology*, 4: Article 59, 2013.

[6] Przekwas A., Somayaji M.R., and Gupta R.K. Synaptic mechanisms of blast-induced brain injury. *Frontiers in Neurology*, 7: Article 2, 2016.

[7] Baker W.E., Cox P.A., Westine P.S., Kulesz J.J., and Strehlow R.A. *Explosion Hazards and Evaluation*, volume 5 of *Fundamental studies in engineering*. Elsevier Scientific Publishing Company, New York, 1983.

[8] Tang M.J. and Baker Q.A. A new set of blast curves from vapor cloud explosion. *Process Safety Progress*, 18:235–240, 1999.

[9] Dewey J.M. *Blast Effects: Physical Properties of Shock Waves*, chapter The Friedlander Equations, pages 37–55. Shock Wave and High Pressure Phenomena. Springer, New York, 2018.

[10] Hydrohub Innovation Program. Safety aspects of green hydrogen production on industrial scale. Public report, Institute for Sustainable Process Technology, The Netherlands, November 2023.

[11] Van den Berg A.C. The multi-energy method - a framework for vapor cloud explosion blast prediction. *Journal of Hazardous Materials*, 12:1–10, 1985.

[12] Tang M.J. and Baker Q.A. Comparison of blast curves from vapor cloud explosions. *Journal of Loss Prevention in the Processes Industries*, 13:433–438, 2000.

[13] Puttock J.S., Yardley M.R., and Cresswell T.M. Prediction of vapour cloud explosions using the SCOPE model. *Journal of Loss Prevention in the Processes Industries*, 13:419–431, 2000.

[14] Puttock J.S. Developments in the Congestion Assessment Method for the prediction of vapour-cloud explosions. In Pasman H.J., Fredholm O., and Jacobsson A., editors, *Loss Prevention and Safety Promotion in the Process Industries, Proceedings of the 10th International Symposium*, pages 1107–1133, Stockholm, Sweden, June 2001. Elsevier.

[15] Dorofeev S.B. Evaluation of safety distances related to unconfined hydrogen explosions. *International Journal of Hydrogen Energy*, 32:2118–2124, 2007.

[16] Van den Berg A.C. A 1-D variable flame speed blast simulation code using a flux-corrected transport algorithm. Report PML 1980-162, TNO Prins Maurits Laboratory, The Netherlands, 1980.

[17] Wiekema B.J. Vapour cloud explosion model. *Journal of Hazardous Materials*, 3:221–232, 1971.

[18] Kinsella K.G. A rapid assessment methodology for the prediction of vapour cloud explosions. Research Report 357, Technical Research Centre of Finland, 1993.

[19] Van der Linden M. and Wolting A.G. Effecten van waterstofexplosies. Public report 2024-0032, National Institute for Public Health and the Environment (RIVM), The Netherlands, 2024.

[20] Baker Q.A., Tang M.J., Scheier E.A., and Silva G.J. Vapor cloud explosion analysis. *Process Safety Progress*, 15:106–109, 1996.

[21] Taylor G.I. The air wave surrounding an expanding sphere. *Proceedings of the Royal Society of London, Series A: Mathematical and Physical Sciences*, 186:273–292, 1946.

[22] Taylor G.I. The formation of a blast wave by a very intense explosion. I. Theoretical discussion. *Proceedings of the Royal Society of London, Series A: Mathematical and Physical Sciences*, 201:159–174, 1950.

[23] Taylor G.I. The formation of a blast wave by a very intense explosion. II. The atomic explosion of 1945. *Proceedings of the Royal Society of London, Series A: Mathematical and Physical Sciences*, 201:175–186, 1950.